EFFECTS OF LOW TEMPERATURES ON STRENGTH AND TIME-DEPENDENT DEFORMATION OF ROCK SALT

Tidarat Khathipphathee

A Thesis Submitted in Partial Fulfillment of the Requirements for the Degree of Master of Engineering in Geotechnology

Suranaree University of Technology

Academic Year 2012

ผลกระทบของอุณหภูมิต่ำต่อความแข็งและการเปลี่ยนรูปร่างเชิงเวลาของเกลือหิน

นางสาวธิดารัตน์ ข่าทิพย์พาที

วิทยานิพนธ์นี้เป็นส่วนหนึ่งของการศึกษาตามหลักสูตรปริญญาวิศวกรรมศาสตรมหาบัณฑิต
สาขาวิชาเทคโนโลยีธรณี
มหาวิทยาลัยเทคโนโลยีสุรนารี
ปีการศึกษา 2555

EFFECTS OF LOW TEMPERATURES ON STRENGTH AND TIME-DEPENDENT DEFORMATION OF ROCK SALT

Suranaree University of Technology has approved this thesis submitted in partial fulfillment of the requirements for a Master's Degree.

Thesis Examining Committee

_____

(Assoc. Prof. Kriangkrai Trisarn)

Chairperson

_____

(Assoc. Prof. Dr. Kittitep Fuenkajorn)

Member (Thesis Advisor)

_____

(Dr. Prachya Tepnarong)

Member

_____ _____

(Prof. Dr. Sukit Limpijumnong) (Assoc. Prof. Flt. Lt. Dr. Kontorn Chamniprasart)

Vice Rector for Academic Affairs Dean of Institute of Engineering

ธิดารัตน์ ข่าทิพย์พาที : ผลกระทบของอุณหภูมิต่ำต่อความแข็งและการเปลี่ยนรูปร่างเชิงเวลาของเกลือหิน (EFFECTS OF LOW TEMPERATURES ON STRENGTH AND TIME-DEPENDENT DEFORMATION OF ROCK SALT) อาจารย์ที่ปรึกษา : รองศาสตราจารย์ ดร.กิตติเทพ เฟื่องขจร, 65 หน้า.

วัตถุประสงค์ของการศึกษานี้ คือ เพื่อหาผลกระทบของอุณหภูมิต่ำต่อการเปลี่ยนรูปร่างเชิงเวลาของเกลือหินซึ่งเตรียมจากเกลือหินชั้นกลางของหมวดหินมหาสารคามในภาคตะวันออกเฉียงเหนือของประเทศไทย โดยทำการทดสอบการคืบในแกนเดียวภายใต้อุณหภูมิคงที่ ที่ 0 องศาเซลเซียสและ 30 องศาเซลเซียส วิธีการทดสอบและการคำนวณได้ดำเนินตามมาตรฐาน ASTM ใช้ระยะเวลาการทดสอบ 21 วันต่อตัวอย่างเกลือหิน เครื่องทำความเย็นถูกประดิษฐ์ขึ้นเพื่อใช้ทดสอบภายใต้อุณหภูมิต่ำ สมการในรูปแบบของ Exponential creep law ถูกใช้อธิบายการเปลี่ยนรูปร่างเชิงเวลาหรือพฤติกรรมของตัวอย่างเกลือหินภายใต้การผันแปรอุณหภูมิ ผลการทดสอบสามารถสรุปได้ว่าการเปลี่ยนรูปร่างของเกลือหินจะเพิ่มขึ้นตามอุณหภูมิที่เพิ่มขึ้น ในช่วงแรกการเปลี่ยนรูปร่างที่ขึ้นกับเวลา (Transient) จะเพิ่มขึ้นตามเวลาและมีแนวโน้มที่จะคงที่ในช่วงที่สองคือช่วงการเปลี่ยนรูปร่างคงที่ (Steady-state) การเปลี่ยนรูปร่างของเกลือหินภายใต้อุณหภูมิต่ำจะน้อยกว่าภายใต้อุณหภูมิห้องประมาณร้อยละ10 การจำลองด้วยโปรแกรมคอมพิวเตอร์ได้ใช้ค่าปัจจัยที่สอบเทียบจากการทดสอบการคืบในแนวแกนเดียว เพื่อประเมินการยุบของโพรงกักเก็บคาร์บอนไดออกไซด์ภายใต้การผันแปรอุณหภูมิ ผลการจำลองระบุว่าการยุบตัวของโพรงกักเก็บภายใต้อุณหภูมิห้อง มีค่าสูงกว่าการยุบตัวของโพรงกักเก็บภายใต้อุณหภูมิต่ำและค่าเสถียรภาพของโพรงกักเก็บภายใต้อุณหภูมิต่ำมีค่าสูงกว่าภายใต้อุณหภูมิห้อง ซึ่งบอกเป็นนัยว่าการประเมินเสถียรภาพของโพรงกักเก็บโดยใช้ผลการทดสอบภายใต้อุณหภูมิห้องจะให้ผลอยู่ในเชิงอนุรักษ์

สาขาวิชา เทคโนโลยีธรณี ลายมือชื่อนักศึกษา _____

ปีการศึกษา 2555 ลายมือชื่ออาจารย์ที่ปรึกษา_____

TIDARAT KHATHIPPHATHEE : EFFECTS OF LOW TEMPERATURES ON STRENGTH AND TIME-DEPENDENT DEFORMATION OF ROCK SALT. THESIS ADVISOR : ASSOC. PROF. KITTITEP FUENKAJORN, Ph.D., P.E., 65 PP.

CARBON DIOXIDE/SEQUESTRATION/SALT CAVERN/CREEP/CARBON EMISSION

The objective of this study is to experimentally determine the effects of low temperatures on the time-dependent deformation of rock salt obtained from the Maha Sarakham formation. Uniaxial creep test is performed under constant temperatures at 0 and 30 Celsius. The test methods and calculation follow the ASTM standard practices. The test duration for the creep testing is 21 days. A cooling system has been fabricated for the low temperature testing. The exponential creep law is used to describe the time-dependent deformations of the salt specimens under various testing temperatures. The test results indicate that the creep deformation increases with the temperatures. The transient creep rate increases with time and tends to be constant at steady-state creep phase. Salt creep under the low temperature is about 10% lower than that under the ambient temperature. The cavern closure predicted from the parameters calibrated from low temperature testing is lower than that under ambient temperature testing. This suggests that evaluation of the stability of CO_2 storage cavern by creep tests under ambient temperature tends to be conservative.

School of Geotechnology Student's Signature_____

Academic Year 2012 Advisor's Signature_____

ACKNOWLEDGMENTS

I wish to acknowledge the funding support of Suranaree University of Technology (SUT).

I would like to express my sincere thanks to Assoc. Prof. Dr. Kittitep Fuenkajorn, thesis advisor, who gave a critical review and constant encouragement throughout the course of this research. Further appreciation is extended to Assoc. Prof. Kriangkrai Trisarn **:** chairman, school of Geotechnology and Dr. Prachya Tepnarong, School of Geotechnology, Suranaree University of Technology who are member of my examination committee. I am grateful Asean Potash mining Company for donating salt core for testing. Grateful thanks are given to all staffs of Geomechanics Research Unit, Institute of Engineering who supported my work.

Finally, I most gratefully acknowledge my parents and friends for all their supports throughout the period of this research.

Tidarat Khathipphathee

TABLE OF CONTENTS

Page

TABLE OF CONTENTS (Continued)

Page

TABLE OF CONTENTS (Continued)

Page

LIST OF TABLES

Table **Page**

LIST OF FIGURES

Figure **Page**

LIST OF FIGURES (Continued)

Figure **Page**

LIST OF FIGURES (Continued)

Figure **Page**

SYMBOLS AND ABBREVIATIONS

$\dot{\varepsilon}_{cr}$	=	Creep rate
κ	=	Creep constant
γ	=	Constant creep parameter
α	=	Constant creep parameter
λ	=	Constant creep parameter
β	=	Constant creep parameter
σ^{-}	=	Deviatoric part of the deviatoric stresses
ϕ	=	Friction angle
ν	=	Poisson's ratio
ε_1	=	Strain in maximum principal stress direction
ε_2	=	Strain in intermediate principal stress direction
ε_3	=	Strain in minimum principal stress direction
σ_B	=	Brazilian tensile strengths
σ_c	=	Uniaxial compressive strengths
ε_m	=	Mean strains
σ_v	=	Vertical stress
A	=	Constant creep parameter
B′	=	Constant creep parameter
c	=	Cohesion

SYMBOLS AND ABBREVIATIONS (Continued)

C	=	Specific heat
E	=	Young's modulus
E_1	=	Elastic modulus
E_2	=	Visco-elastic parameter
G	=	Shear modulus
K	=	Bulk modulus
k	=	Thermal conductivity
m	=	Constant creep parameter
n	=	Constant creep parameter
T	=	Temperature (Kelvin)
t	=	Time
γ_{oct}	=	Octahedral shear strain
ρ	=	Rock Density
σ_1	=	Maximum Principal Stress
σ_3	=	Minimum Principal Stress
σ_m	=	Mean stress
τ_{oct}	=	Octahedral Shear Stress
η_1	=	Visco-plastic Parameter
η_2	=	Visco-elastic Parameter
σ_2	=	Intermediate principal Stress

CHAPTER I

INTRODUCTION

1.1 Background and rationale

Geological sequestration of CO_2 is a mitigation option for reducing CO_2 emissions into the atmosphere that is immediately available and technologically feasible. The technology has already been developed and applied for underground storage of petroleum, natural gas and compressed air (Tek 1989; Bradley et al., 1991) or for salt mining. Sequestration of CO_2 in salt caverns differs from natural gas storage in terms of time scale, and the long-term behavior of the salt cavern, and hence requires investigating in terms of permanency and safety of the operation. Storage of fluids in crustal caverns often requires cryogenic conditions to keep such fluids in a condensed state and maximize storage capacity. Durham et al. (2008) study the behavior of salt caverns in the presence of cryogenic fluids. They have carried out a series of laboratory creep experiments on samples of Waste Isolation Pilot Project, New Mexico and Avery Island (Gulf of Mexico) rock salt samples at temperatures from 100 to 300 Kelvin. Test conditions assured that the deformation was in the ductile field. All samples displayed work hardening and even the coldest samples responded with some amount of permanent deformation, roughly 2% in four days in the case of samples deformed at highest stress and lowest temperature. Work hardening behavior, resolvable at T > 160 Kelvin suggests a useful universal work hardening law that relates microstructure to strain, independent of applied stress or

strain rate. The study to evaluate the ability of salt caverns to creep behavior to relieve large thermally induced stresses without losing integrity, data are needed on the plasticity of rock salt under temperatures ranging from 0 to 30 Celsius or under CO_2 storage condition.

1.2 Research objectives

The objective of this study is to experimentally determine the effects of low temperatures on the time-dependent deformation of rock salt obtained from the Maha Sarakham formation. Laboratory testing includes the uniaxial creep tests performed under twos temperatures ranging from 0 and 30 Celsius. A finite difference code (FLAC) is used to simulate the deformability of CO_2 storage cavern under low temperatures, using the salt properties calibrated from the creep tests. A constitutive relation between the mechanical loadings and the creep deformation of the salt under varied temperatures is derived. The results are used to determine the salt cavern stability under CO_2 storage condition.

1.3 Research methodology

The research methodology shown in Figure 1.1 comprises 7 steps; including literature review, sample preparation, laboratory testing, simulation, discussions and conclusions and thesis writing.

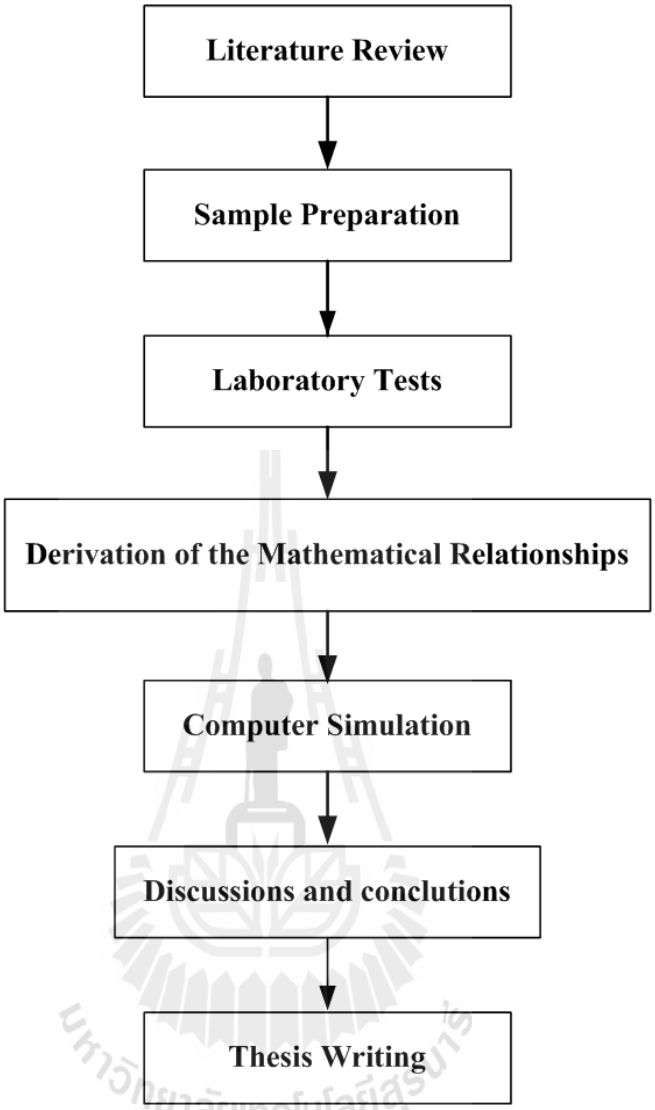

Figure 1.1 Research methodology

1.3.1 Literature review

Literature review is carried out to study the previous researches on time-dependent behavior of rock salt as affected by the mechanical and thermal loadings. The sources of information are from text books, journals, technical reports and conference papers.

1.3.2 Sample preparation

Rock salt samples have been donated by Asean Potash Mining Co. from the Khorat basin, northeast of Thailand. The salt cores belong to the Middle salt member of the Maha Sarakham formation. Nine samples are prepared for uniaxial creep test. The salt specimens are cylindrical shaped with 100 mm in diameter and 250 mm in length (L/D=2.5). Preparations of these samples follow as much as practical the American Society for Testing and Materials (ASTM D4543).

1.3.3 Laboratory Testing

Laboratory tests include uniaxial creep test under ambient and low temperatures. A consolidation loading frame is used to apply constant axial stresses to the cylindrical salt specimens. The control axial stresses are 6.5, 9.6, 13.0, 14.8 and 16.0 MPa.

1.3.4 Derivation of the Mathematical Relationships

The test results are used to determine the deformability and strength of salt rock specimens, elastic modulus, Poisson's ratio, and stress-strain with time dependency under ambient and low temperatures.

1.3.5 Computer simulations

The creep parameters calibrated from various cases are used to assess the stability of carbon dioxide storage caverns by using the finite difference code (FLAC 4.0). A finite difference analysis is performed for various cavern geometries to demonstrate the impact of the low temperatures on the salt behavior around the storage caverns.

1.3.6 Conclusion and thesis writing

The researched findings is discussed and analyzed to determine the impacts of the thermal and mechanical loads on the storage cavern stability. All research activities, methods, and results are documented and complied in the thesis. The research or findings is published in the conference proceedings or journals**.**

1.4 Scope and limitations

The scope and limitations of the research include as follows.

1. All testing are conducted on rock salt specimens obtained from the Maha Sarakham formation.

2. The uniaxial creep tests are performed with the applied axial stresses varying from 30 to 50 percents of the salt strength. Testing temperatures for the uniaxial creep testing range from 0 to 30 Celsius.

3. All creep tests are performed up to 21 days

4. All testing are made under dry condition.

5. Numerical simulations using FLAC are performed to study the salt creep.

1.5 Thesis contents

This research thesis is divided into seven chapters. The first chapter includes background and rationale, research objectives, research methodology, and scope and limitations. **Chapter II** presents results of the literature review to improve an understanding of rock salt on time-dependent behavior under temperatures. **Chapter III** describes the sample preparation and laboratory tests. **Chapter IV** presents creep parameters results from calibration. **Chapter V** presents results computer simulations. **Chapter VI** is the discussions, conclusions and recommendations for future studies.

CHAPTER II

LITERATURE REVIEW

2.1 Introduction

This chapter summarizes the results of literature review carried out to improve an understanding of rock salt behaviour under temperatures and strength.

2.2 Salt behavior

The time-dependent deformation (or creep) is the process at which the rock can continue deformation without changing stress. The creep strain seldom can be recovery fully when loads are removed, thus it is largely plastic deformation. Creep deformation occurs in three different phases, as shown in Figure 2.1, which relatively represents a model of salt properties undergoing creep deformation due to the sustained constant load. Upon application of a constant force on the rock salt, an instantaneous elastic strain (ε_e) is induced. The elastic strain is followed by a primary or transient strain, shown as Region I. Region II, characterized by an almost constant slope in the diagram, corresponds to secondary or steady state creep. Tertiary or accelerating creep leading to rather sudden failure is shown in Region III. Laboratory investigations show that removal of applied load in Region I at point L will cause the strain to fall rapidly to the M level and then asymptotically back to zero at N. The distance LM is equal to the instantaneous strain ε_e. No permanent strain is induced here. If the removal of stress takes place in the steady-state phase the permanent

strain (ε_p) will occur. From the stability point of view, salt structure deformations after constant load removal have only academic significance, since the stresses imposed underground due to mining operations are irreversible. The behavior of the salts with time-dependent deformation under constant load is characterized as a visco-elastic and visco-plastic phenomenon. Under these conditions the strain criteria are superior to the strength criteria for design purposes, because failure of most salt pillars occurs during accelerated or tertiary phase of creep, due to the almost constant applied load.

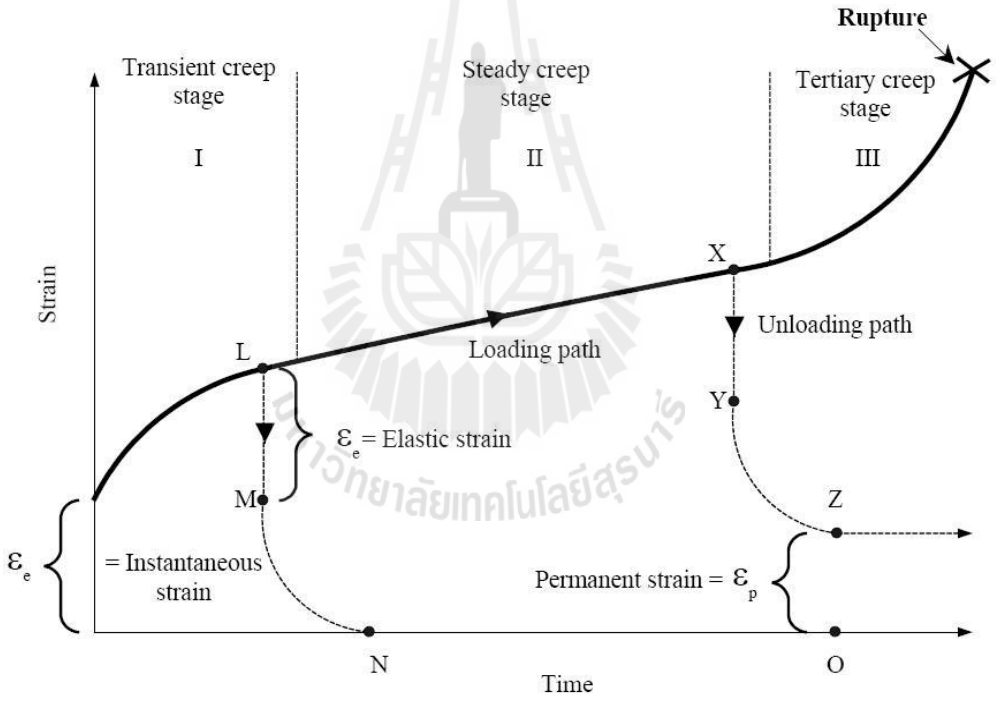

Figure 2.1 The typical deformation as a function of time of creep materials (modified from Jeremic, 1994).

The dimensions of a pillar in visco-elastic and visco-plastic rock should be established on the basis of a prediction of its long-term strain, to guard against adequate safety factor accelerating creep (Fuenkajorn and Daemen, 1988; Dusseault and Fordham, 1993; Jeremic, 1994; Knowles et al., 1998).

The Burgers model is one of linear visco - elastic models. These models yield a linear relationship between stress (σ) and strain rate ($\varepsilon(t)$ or $\partial\varepsilon/\partial t$) as follows (Coleman and Noll, 1961; Gnirk and Johnson, 1964):

$$\sigma + \left(\frac{\eta_1}{E_1} + \frac{\eta_2}{E_2} + \frac{\eta_1}{E_2}\right)\dot{\sigma} + \frac{\eta_1\eta_2}{E_1E_2}\ddot{\sigma} = \eta_1\dot{\varepsilon} + \frac{\eta_1\eta_2}{E_2}\ddot{\varepsilon} \qquad (2.1)$$

The Burgers models describe equations for uniaxial constant stress, constant stress rate and constant rate testing. The derivation is made by using a Laplace transformation. For uniaxial constant stress, visco - elastic are presented as function of constant axial stress (σ_0), time and spring and dashpot constant shown in Figure 2.2 and equations (2.2) as follows:

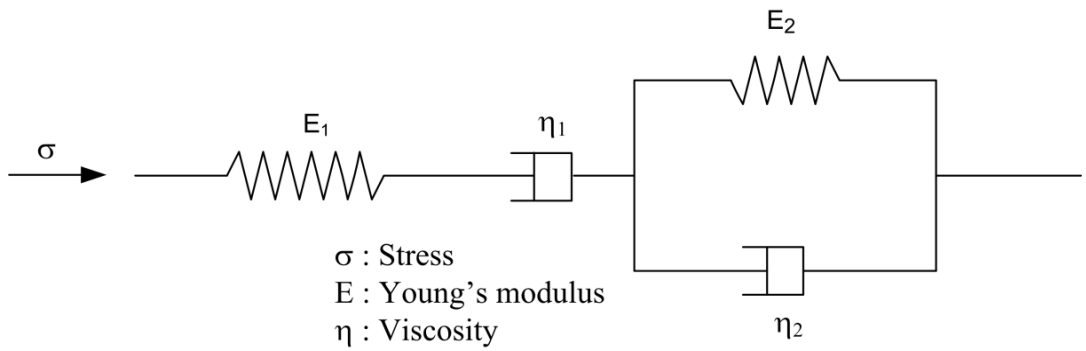

Figure 2.2 Burgers model built up of combinations of linear spring and dashpots. (Jeager and Cook, 2007)

$$\varepsilon(t) = \sigma_0 \left\{ \frac{1}{E_1} + \frac{t}{\eta_1} + \frac{1}{E_2} \left[1 - \exp\left(- E_2 t / \eta_2 \right) \right] \right\} \tag{2.2}$$

Yanan et al. (2010) propose the constitutive models of rock as affected by temperature and humidity. Based on the Nishihara model, a visco-elastic-plastic rock model was established by using the coefficients of thermal and humidity expansion, thermal viscosity attenuation, humid viscosity attenuation and acceleration rheology components. They used the definition of a controlled heat circle to explain the model. The results show that the behavior of rock, affected by temperature and humidity, is stable as a function of time when the stress is lower than the first yield stress (σ_{S1}). The creep rate will increase due to the effect of temperature and humidity when the stress is greater than or equal to the first yield stress (σ_{S1}), the creep rate will accelerate at an increasing rate when the stress is greater than or equal to the second yield stress (σ_{S2}) shown in Figure 2.3.

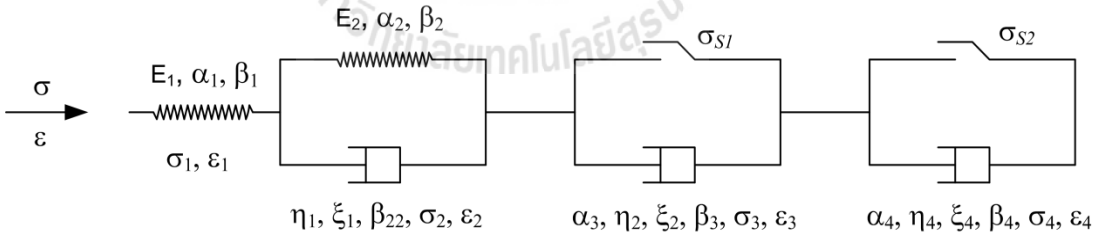

Figure 2.3 Visco-elastic-plastic constitutive models with temperature-humidity effects (Yanan et al., 2010).

In Figure 2.3, E_1, E_2 are the stiffness coefficients of springs, α_1, α_2 are the thermal expanding coefficients of springs, β_1, β_2 are the humidity expanding coefficients of springs and β_{22}, β_3, β_4 the humidity attenuation coefficients of dashpots. η_1, η_2, η_3 are viscosity parameters and ξ_1, ξ_2, ξ_3 the temperature attenuation coefficients of dashpots. σ_{S1} is the first yield stress which is the threshold value of the increasing creep rate and σ_{S2} is the second yield stress, i.e., the threshold value of accelerated creep. *T*, *W* are temperature and humidity respectively.

If $\sigma < \sigma_{S1}$, the model is composed of a spring and a Kelvin element, hence:

$\varepsilon = \varepsilon_1 + \varepsilon_2, \varepsilon \xrightarrow{t\to\infty} 0$, the creep deformation of the wall rock will be stable. If $\sigma_{S1} \leq \sigma < \sigma_{S2}$, the model is composed of a spring, a Kelvin element and an ideal visco - plastic element, hence: $\varepsilon = \varepsilon_1 + \varepsilon_2 + \varepsilon_3, \dot{\varepsilon} \xrightarrow{t\to\infty} \beta_3 W + \xi_2 T + \frac{\sigma_0 - \sigma_{S1}}{\eta_2}$, the creep rate of the wall rock will increase remain constant at a constant value. If $\sigma \geq \sigma_{S2}$, the model is composed of a spring, a Kelvin element and an ideal visco-plastic element and an acceleration rheology component, $\varepsilon \xrightarrow{t\to\infty} \beta_3 W + \xi_2 T + \frac{\sigma_0 + \sigma_{S1}}{\eta_2} t$, the creep rate will accelerate at a constant rate and failure will occur, which results in a failure of the roadway. The model derived in this study can completely describe visco - elastic-plastic characteristics and reflects the three stages of rock creep.

Langer (1984) and Farmer (1983) present numerous empirical equations describing the time - dependent behavior of geological materials. Two types of empirical laws that explicitly contain creep strain, stress, and time variables are selected for use this investigation potential laws and exponential laws. The laws are applied to describe salt behavior without considering the actual mechanism of deformation. Generally, empirical constitutive model are developed by linking the creep strain to stress and temperature. The potential laws are power equations relating

creep strain, stress, time and temperature. Two empirical models describing transient and steady – state creep strains can be expressed as:

$$\varepsilon(t) = K'\sigma^{\beta}t^{\gamma}T^{\alpha} \quad \text{(transient)} \tag{2.3}$$

$$\dot{\varepsilon}(t) = A'\sigma^{B}T^{C} \quad \text{(steady – state)} \tag{2.4}$$

The exponential laws present the transient creep strain as a function of stress, time and temperature in exponential form:

$$\varepsilon(t) = B'\sigma^{m}t^{n}\exp(-\lambda/T) \tag{2.5}$$

where $\varepsilon(t)$ is transient creep strain, $\dot{\varepsilon}(t)$ is steady – state creep strain rate, σ is stress, t is time, T is absolute temperature, K′, α, β, γ, A′, B, C, B′, m, n, λ is empirical constants.

Charpentier (1984) study the time-dependent behavior of rock salt under temperature has guided the "Laboratorie de Mecanique des Solides" to develop specific creep equipment. The design and capacity of this creep test installation offer the possibility of studying a wide range of materials. Considering the characteristics of the problem the "Laboratorie de Mecanique des Solides" has designed a specific creep equipment to carry out long term at high temperature. At present, the experimental installation of three temperature levels between 20°C and 200°C for uniaxial creep. The specimens used are cylinders of 7 cm in diameter and 16 cm in height on Bresse salt. Two specimens test at 20°C applies the uniaxial stresses of 15.3 MPa and 17.8 MPa correspond respectively to 65% and 75% of the uniaxial

compressive strength. The creep was observed during two months. At this stage the strain rate is not stable yet and they are still in a transient phase for the two samples. This primary creep can be interpreted by means of a time – hardening law. Test at 100°C applies the uniaxial stresses of 11.3 MPa and 15.3 MPa correspond respectively to 65% and 75% of the uniaxial compressive strength. During about 30 days the values of $\dot{\varepsilon}$ are 13×10^{-6} hr^{-1} and 18×10^{-6} hr^{-1}. For the most severely loaded sample, the increase of the strain rate after two months denotes the existence of a tertiary state which can probably lead to failure. Three specimens obtained on test at 200°C. The uniaxial stresses of 3.4 MPa, 5 MPa and 7.5 MPa correspond respectively to 20%, 30% and 45% of the uniaxial compressive strength. For the two specimens with the highest levels of load the creep is very important, the strains are 15% and 25% after about two months. This fact shows the major effect of temperature on the time-dependent behavior of rock salt. For the specimens with the smallest load, they have measured only 2% of strain after two months. This difference leads us to consider a yielding point for the behavior law of our rock salt.

Temperature or heating affects the creep deformation, because they increase the plastic property of salt and long-term deformation (Pudewills et al., 1995). Jeremic (1994) postulates that rock salts lose their brittleness after extension tempering at approximately 600 °C and exhibit a critical shear stress up to 1 MPa. Hamami et al. (1996) study the effect of temperature and conclude that the temperature increase, as for the deviatoric stress, results in an increase of the material deformation. Cristescu and Hunsche, (1996) study the temperature effect on the strain rate suitable for laboratory testing. They suggest that the appropriate strain rate for

testing at 100 °C and 200 °C is 10^{-8} s^{-1} and 10^{-7} s^{-1} because the temperature can affect the creep deformation and strength of salt under high temperatures.

Inada et al. (1997) study the temporary storage of high and low temperature materials in openings excavated in rock mountain from the view point of efficient utilization of land and preservation of the environment. In this case, high temperature materials means such as heated water which is produced by surplus heat from garbage burning plants, and low temperature materials means such as LNG, LPG, frozen food etc. Heated water, LNG and LPG actually are stored in openings, as the quantity of these materials changes continually, the rock mass around openings will receive the effects of thermal hysteresis of high and low temperatures. Therefore, obtaining the strength and deformation characteristics of rock after undergoing thermal hysteresis of high and low temperatures becomes important for discussing the stability of the openings. In this study, strength and deformation characteristics of rock which has low and high porosity were examined after undergoing thermal hysteresis of high and low temperatures using a thermal cycle apparatus. From the results, it was found that temperature, the number of hysteresis and porosity etc. were important factors which have an influence on strength and deformation characteristics. The main results obtained in this study are as follows is compressive and tensile strength of rocks decrease with the increasing number of thermal hysteresis. However, the ratio of decreasing decreases. From this fact, it is supposed that the value will converge to a constant value. The values of tangential Young's modulus and Poisson's ratio of rocks after undergoing thermal hysteresis have the same tendency as those of compressive and tensile strength. From the results of measuring strain, the residual strains at room temperature can be seen for all specimens after undergoing thermal hysteresis.

However, it is considered that the residual strain tends to converge to a constant value as thermal hysteresis is repeated. Elastic wave propagation velocity of rocks decreases with the increasing number of thermal hysteresis, but the ratio of decreasing decreases. It is considered that the value will converge to a constant value.

Yang and Daemen (1997) investigate the temperature effects on creep of tuff. Creep tests have been conducted at room temperature and at elevated temperature (204 °C). In order to model the creep behavior of tuff, a new time-dependent damage model and two definitions of stress intensity factor are proposed. The results of experiments and theoretical analysis show that the creep strain of tuff increases with increasing temperature under the same loading condition, and that the stress intensity factor is not only a function of stress states, but also of temperature.

Pudewills and Droste (2003) study the numerical simulation of the thermal and thermomechanical response of the large-scale in situ experiment ‘‘thermal simulation of drift emplacement’’, which was carried out in the Asse salt mine in Germany. The analyses concern the modeling of the temperature fields, thermally induced drift closure followed by the consolidation of backfill material and the distribution of the stresses. Finite element codes (ADINA and MAUS) specially developed for the repository structures as well as a general-purpose code have been used. The primary objective of the investigations is to evaluate the capability of these codes to simulate the thermomechanical behavior of rock salt and backfill material under representative conditions of a waste repository by comparing of calculated results with in situ measurements. An overall good agreement between modeling and in situ measured results indicates that most thermomechanical effects are fairy well represented by the numerical models.

The thermomechanical behavior of rock salt was described in the finite element analyses by a thermoelastic material model with a temperature-dependent steady- state creep and based on the experimental results. According to this model, the total strain rate is given as the sum of elastic, thermal, and steady-state creep rates. This constitutive relation governing the creep strain rate of rock salt is described as follows:

$$\varepsilon_{ef} = A\sigma^{5}_{ef} \exp(-Q/(RT)) \quad (2.6)$$

Dwivedi et al. (2008) study the thermo-mechanical and transport properties of granites which is required to understand and model a number of processes in the earth crust such as folding, geothermal activity, magmatic intrusions, plate tectonics and nuclear waste disposal. Thermo-mechanical properties of Indian granite (IG) is studied various at high temperatures in the range of 30–160 °C, keeping in view the highest temperatures expected in underground nuclear waste repositories. These properties are Young's modulus, uniaxial compressive strength, tensile strength, Poisson's ratio, coefficient of linear thermal expansion, creep behaviour and the development of micro-crack on heating using scanning electron microscope (SEM). The results indicate that the temperature effect on creep under atmospheric pressure condition (0.1 MPa) was not observed up to 160 °C in the duration of 4 months for Indian pink granite. Permeability decreases with increase in temperature. Thermal conductivity and thermal diffusivity both decrease with increase in temperature. The decrease in thermal conductivity with temperature is high on increase of the confining pressure. On the other hand, specific heat increases with increase in temperature and

pressure up to 600 °C and the coefficient of linear thermal expansion increases with temperature up to 470 °C. Viscosity of molten granite decreases with increase in temperature. Ultimate compressive strength increases with increase in confining pressure. On the other hand, tensile strength of all granites decreases with increase in temperature for the reported temperature range 30–1050 °C. Normalized cohesion (c/c_0) and normalized angle of internal friction (ϕ/ϕ_0) both decrease with increase in temperature for all granites.

Bachu and Dusseault (2005) propose the salt characteristics and behavior of the Middle Devonian Elk Point Group in the Alberta basin in western Canada, these salt beds are found at depth that range from several hundred meters to more than 2000 meter. The salt beds range in thickness from several tens to a few hundred meters. The vertical stress (weight of the overburden) at the top of these salt beds ranges from 10 to 50 MPa, and temperatures vary between 20 and 70°C. Stresses are assumed to be isotropic and equal to the lithostatic (overburden) within the salt beds, because salt visco plastic properties and slow creep tend to dissipate shear stresses. Vertical stress gradients at the top and bottom of the salt beds are in the 24–25 kPa/m range, and differ by only 0.1–0.3 kPa/m between the two, indicating that they are basically constant across the entire rock package containing the salt beds. If a salt cavern is filled with a fluid at an initial pressure, in the long term the pressure inside the cavern will change as a result of any of: (1) salt creep, (2) leakage along the well bore, (3) thermal expansion of the cavern fluid, (4) flow of the fluid out of the cavern into the adjacent strata, or (5) additional salt solution or precipitation in the cavern (Berest et al., 2000).

Phueakphum and Fuenkajorn (2010) perform cyclic loading tests on the Maha Sarakham salt. Their results indicate that the salt compressive strength decreases with increasing number of loading cycles, which can be best represented by a power equation. The salt elastic modulus decreases slightly during the first few cycles, and tends to remain constant until failure. It seems to be independent of the maximum loads. Axial strain–time curves compiled from loci of the maximum load of each cycle apparently show a time-dependent behavior similar to that of creep tests under static loading. In the steady-state creep phase, the visco-plastic coefficients calculated from the cyclic loading test are about an order of magnitude lower than those under static loading. The salt visco-plasticity also decreases with increasing loading frequency. Surface subsidence and cavern closure simulated using parameters calibrated from cyclic loading test results are about 40% greater than those from the static loading results. This suggests that application of the property parameters obtained from the conventional static loading creep test to assess the long-term stability of storage caverns in salt with internal pressure fluctuation may not be conservative.

Sriapai et al. (2012) study of the temperature effects on salt strength by incorporating empirical relations between the elastic parameters and temperatures of the tested specimens to describe the distortional strain energy density of rock salt under different temperatures and deviation stresses. The results are obtained under temperatures ranging from 273 to 467 Kelvin. Laboratory tests induce the compressive strength and Brazilian tensile strength testing under evaluated temperatures and the results tests show in Table 2.1 – 2.3.

Table 2.1 Uniaxial Compressive Strengths of Salt (Sriapai et al. 2012)

Specimen no.	ρ (g/cc)	Temperature (Kelvin)	σ_c (MPa)
UCS 45-47	2.12 ± 0.03	277.0 ± 2.3	37.9 ± 3.0
UCS 81,87,90	2.00 ± 0.05	298.0 ± 0.6	37.0 ± 2.5
UCS 51-53	2.10 ± 0.01	394.0 ± 4.7	30.0 ± 3.5
USC 74	2.15	455.5	25

Table 2.2 Triaxial Compressive Strengths of Salt (Sriapai et al. 2012)

σ_3 (MPa)	σ_1 (MPa) Testing Temperature			
	274 K	280 K	404 K	467 K
1.6	49.0	45.9	-	-
3	63.6	60.9	52.5	-
5	77.9	76.8	65.6	50.0
10	96.6	93.0	80.6	67.4
15	109.5	105.0	88.9	77.1
20	118.6	113.3	96.0	83.9
30	135.0	128.5	111.0	97.1

Table 2.3 Brazilian Tensile Strengths of Salt (Sriapai et al. 2012)

Specimen no.	ρ (g/cc)	Temperature (Kelvin)	σ_B (MPa)
BZ 1-10	2.12 ± 0.01	274.0 ± 3.1	7.3 ± 0.51
BZ 11-20	2.10 ± 0.05	297.5 ± 0.8	6.0 ± 0.60
BZ 21-30	2.21 ± 0.04	393.7 ± 5.1	5.8 ± 0.84
BZ 31-40	2.09 ± 0.04	464.7 ± 4.5	4.8 ± 0.42

The decrease of the salt strength as the temperature increases suggests that the applied thermal energy before the mechanical testing makes the salt weaker. The temperatures effect is larger when salt is under higher mean stress. To determine the temperature dependency of the failure stress and strain and elastic properties, the strain energy density concept is applied. Assuming that the salt is linearly elastic before failure, the distortional strain energy (W_d) at failure can be calculated as a function of mean strain energy, W_m. For a given W_m, the W_d decreases with increasing temperature. The proposed criterion can be used to determine the stability of rock salt around compressed-air or gas storage caverns during product injection (high temperature, low deviatoric stress) and withdrawal (low temperature, high deviatoric stress). The effect of temperature on the salt strength may be enhanced for the salt cavern with high frequency of injection-retrieval cycles. To be conservative the maximum temperature (induced during injection) and the maximum shear stresses (induced during withdrawal) in salt around the cavern should be determined (normally by numerical simulation). The salt stability can be determined by comparing the computed temperature distribution and mechanical and thermal stresses against the criterion proposed above. The results should lead to a conservative design of the safe maximum and minimum storage pressures.

CHAPTER III

LABORATORY TESTS

3.1 Introduction

The objective of this chapter is to experimentally determine the time-dependent properties of the Maha Sarakham salt under ambient and low temperatures. The sample preparation and specifications of the tested rock salt specimens are described. The laboratory works include uniaxial creep tests under ambient and low temperatures. This chapter describes the test method and results.

3.2 Sample Preparations

Rock salt samples have been donated by Asean Potash Mining Co. from the Khorat basin, northeast of Thailand. The salt cores belong to the Middle salt member of the Maha Sarakham formation. The salt specimens are prepared to obtain cylindrical shaped with 100 mm in diameter and 250 mm in length (L/D=2.5). Preparations of these samples follow as much as practical the American Society for Testing and Materials (ASTM D4543). Table 3.1 summarizes the specimen depth, dimensions and density. The average density is 2.2 ± 0.2 g/cm^3

Figure 3.1 Cutting machine used to prepare salt specimens for this study.

Figure 3.2 Some cylindrical salt specimens prepared for the uniaxial creep test.

Table 3.1 Specimen dimensions prepared for uniaxial creep test.

Sample No.	Depth (m)	Diameter (mm)	Length (cm)	L/D	Weight (g)	Density (g/cc)
UC-01	70.56-70.85	100.6	250.9	2.5	4450.2	2.23
UC-02	70.86-71.11	100.3	252.3	2.5	4450.6	2.23
UC-03	71.16-71.40	101.0	254.2	2.5	4410.5	2.16
UC-04	75.65-75.91	100.7	256.4	2.5	4425.8	2.16
UC-05	76.00-76.26	100.5	255.3	2.5	4465.9	2.20
UC-06	76.27-76.53	100.6	250.1	2.4	4470.6	2.24
UC-07	77.23-77.49	100.3	254.5	2.5	4455.9	2.21
UC-08	78.01-77.76	100.4	252.4	2.5	4412.5	2.23
UC-09	79.52-79.78	100.5	256.6	2.4	4499.5	2.21

3.3 Uniaxial Creep Tests

3.3.1 Consolidation load frame

A consolidation load frame has been used to apply constant axial stress to cylindrical rock specimens (Jandakaew, 2007). The consolidation load frame has been used in this study because the cantilever beams with pre-calibrated dead weight can apply a truly constant axial stress to specimen (Figure 3.3). Dead weight loading devices are used to apply constant axial loads to the specimens. During the test the axial deformation was monitored with two digital gages, each placed on opposite side of the specimen.

Figure 3.3 The consolidation load frame.

3.3.2 Cooling System

A cooling system is fabricated to test the salt cylindrical sample while loading. It can cool the salt specimens down to 0 Celsius. Cooling system consists of compressor, cool coils, hot coils, expansion value and refrigerant (Figure 3.4). The cooling machine is a compressor of 220 – 240 volt 50 Hz and a refrigerant is R134a. After installed the specimen into cooling system will start machine (0°C) until 24 hr before test without loading.

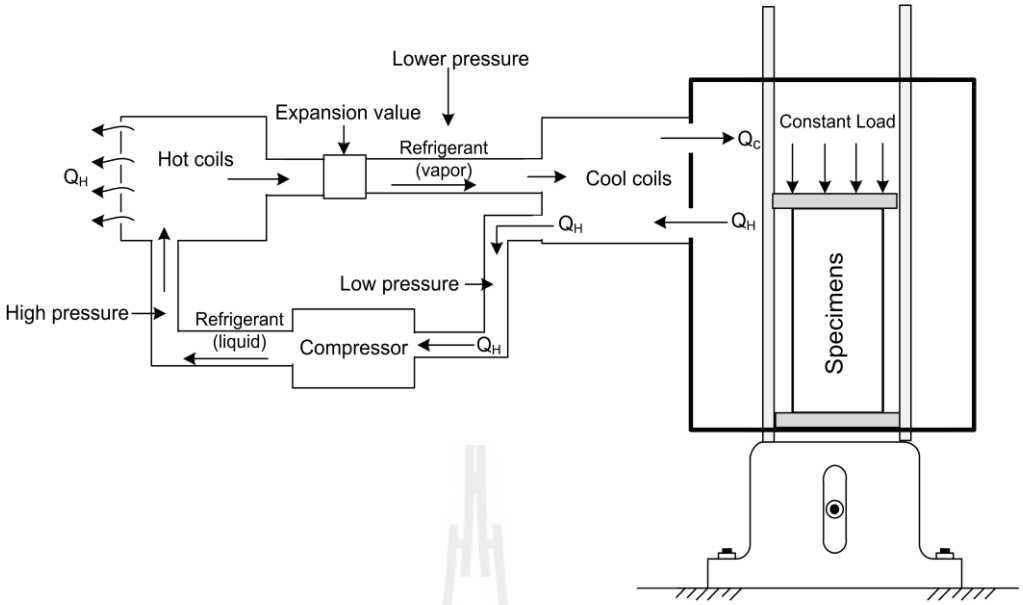

Figure 3.4 Cooling system.

3.3.3 Test method

The uniaxial creep test procedure and apparatus follow the ASTM (D7070) standard practice as much as practical. The salt specimens are installed into the consolidation load frame to provide constant axial stresses. The axial load is pre-calibrated with an electronic load cell to obtain an equivalent axial stress on the specimens. The applied constant axial stresses are 6.5, 9.6, 13.0, 14.8 and 16.0 MPa (about 20% to 50% of the uniaxial compressive strength). The specimen deformations are monitored along the three principal axes for up to 21 days. During the test, the axial and lateral deformations are monitored. The specimen deformations are monitored using four dial gages with high precision (±0.01 mm). The low temperature testing uses the same device as the ambient temperature testing. The samples of low temperatures are installed in a cooling system for 24 hr before start loading. Figure 3.5 shows the specimen placed in the cooling system for low temperature test at 0°C and Figure 3.6 shows the room temperature testing.

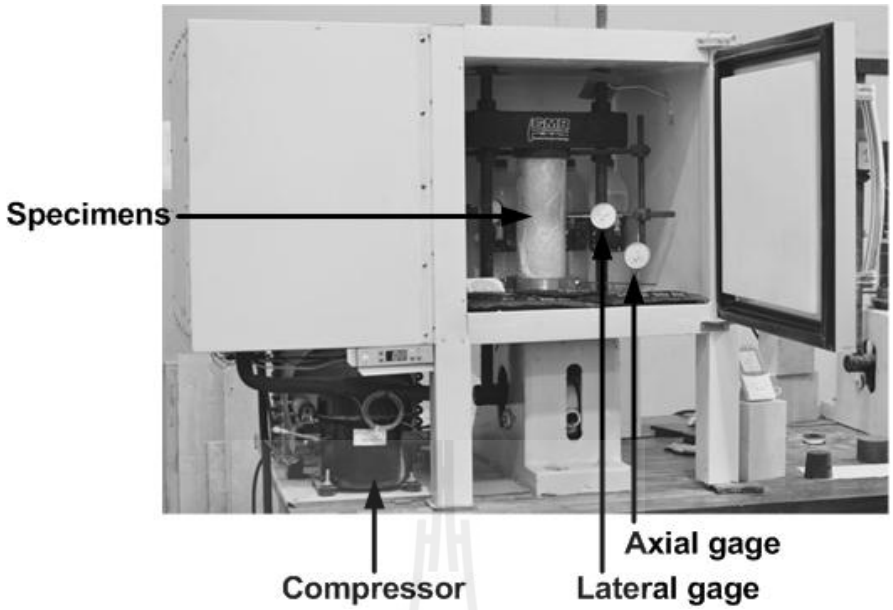

Figure 3.5 Salt specimen placed in the consolidation load frame and inside the cooling system for low temperature test at 0°C.

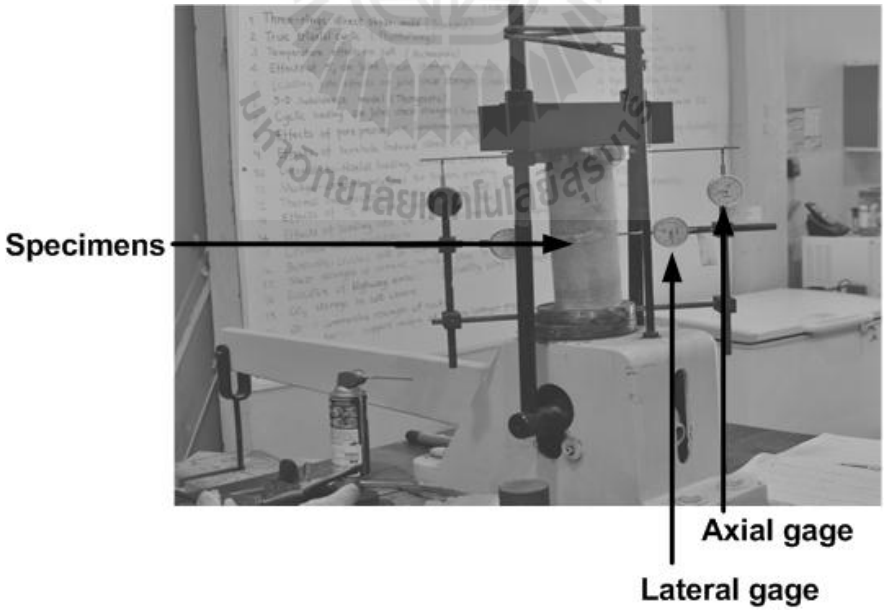

Figure 3.6 Salt specimen placed in consolidation loading frame under room temperatures (about 30°C).

3.3.4 Test Results

Figures 3.7 and 3.8 show the axial and lateral strain-time curves of salt specimens with constant axial stresses range from 6.5 to 16 MPa under low and ambient temperatures. Each salt specimen shows maximum and minimum of instantaneous deformation, transient creep phase and steady-state creep phase.

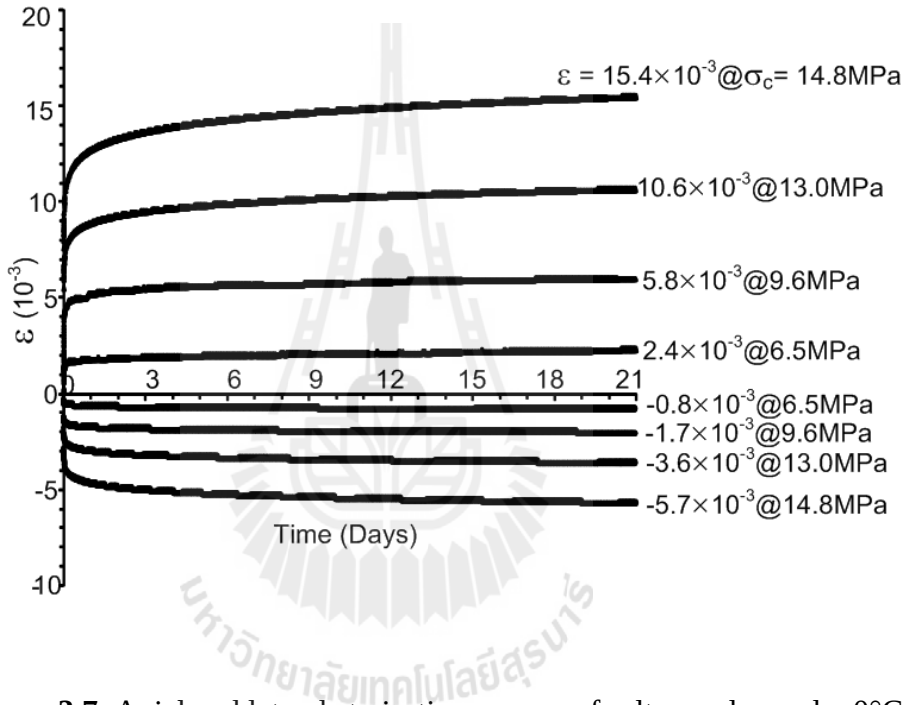

Figure 3.7 Axial and lateral strain-time curves of salt samples under 0°C.

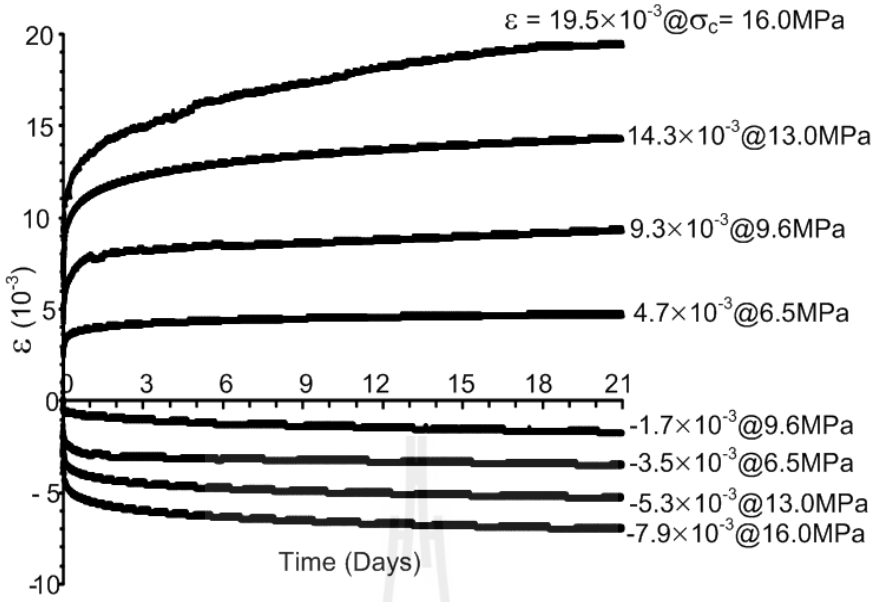

Figure 3.8 Axial and lateral strain-time curves of salt samples under 30°C.

The octahedral shear strains (γ_{oct}) and mean strain (ε_m) can be determined from the test results by the following relations (Jaeger et al., 2007):

$$\gamma_{oct} = 1/3[((\varepsilon_1 - \varepsilon_2)^2 + (\varepsilon_1 - \varepsilon_3)^2 + (\varepsilon_2 - \varepsilon_3)^2)]^{1/2} \quad (4.1)$$

$$\varepsilon_m = \frac{1}{3}(\varepsilon_1 + \varepsilon_2 + \varepsilon_3) \quad (4.2)$$

where γ_{oct} is the octahedral shear strains, ε_m is the mean strains, ε_1, ε_2 and ε_3 are the major, intermediate and minor principal strains measured during the tests ($\varepsilon_{axial} = \varepsilon_1$). Here the intermediate and minor principal strains are equal ($\varepsilon_{lateral} = \varepsilon_2 = \varepsilon_3$). The calculated octahedral shear strains under low and ambient temperature are plotted as a function of time in Figures 3.9 and 3.10 respectively. Figures 3.11 and 3.12 show the

mean strains plotted as function of time with salt specimens with constant axial stresses ranging from 6.5 to 16 MPa under low and ambient temperatures.

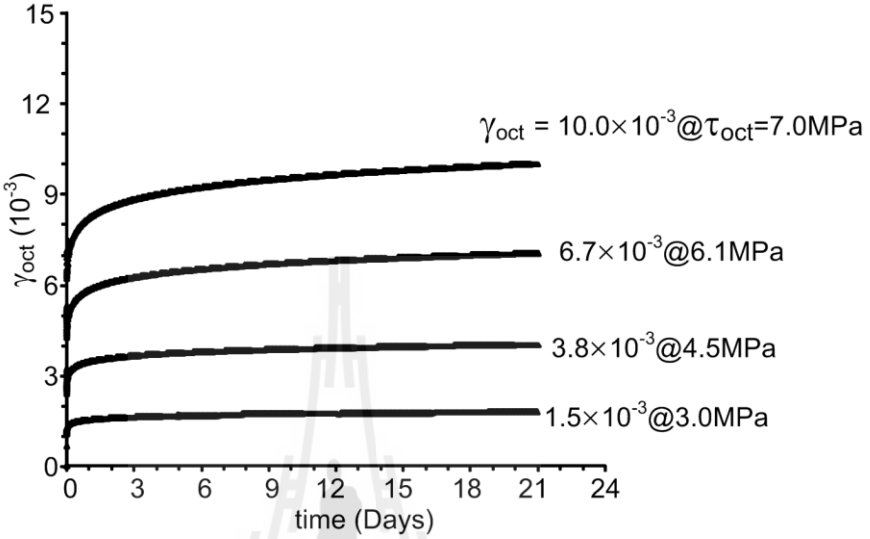

Figure 3.9 Octahedral shear strain-time curves under at 0°C.

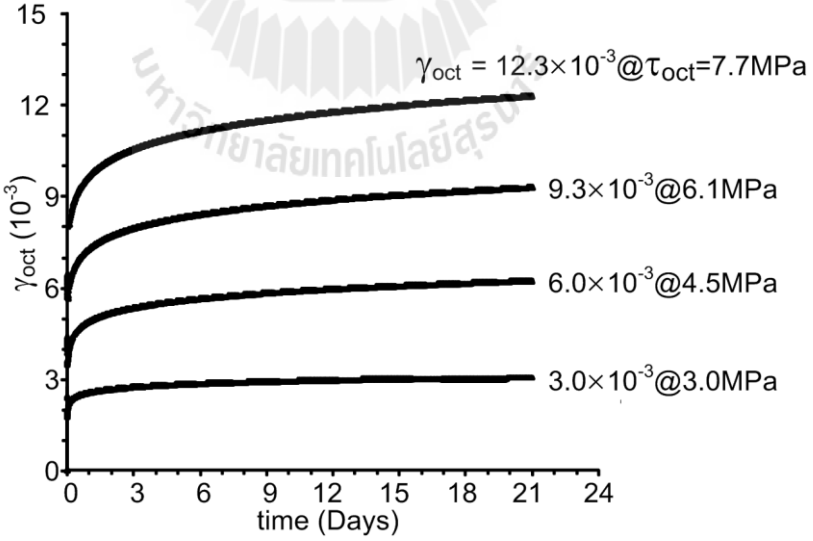

Figure 3.10 Octahedral shear strain-time curves under at 30°C.

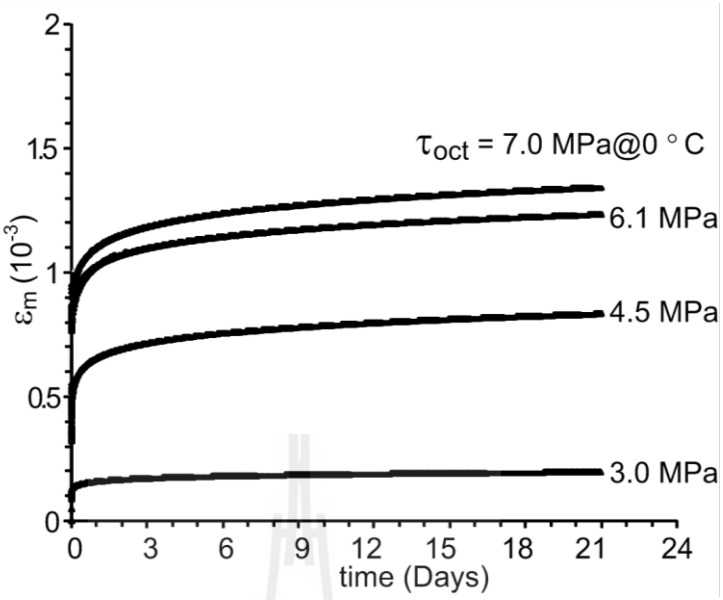

Figure 3.11 Mean strain-time curves for under 0°C.

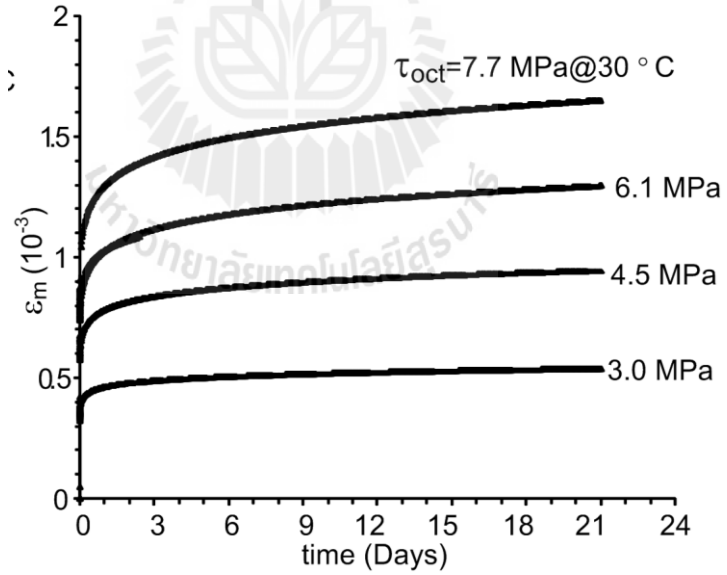

Figure 3.12 Mean strain-time curves for under 30°C.

3.3.4 Discussions

The test results show that the axial strain decreases with increasing the octahedral shear stresses. The transient creep rate of low and ambient temperatures decreases with time, and tend to be constant in steady-state creep phase. Higher creep strains are observed from the room temperatures test results consistent with the temperature or heating that affects the creep deformation. The decrease of the salt strength as the temperatures increases suggests that the applied thermal energy before the mechanical testing makes the salt weaker, and more plastic at lower stress and higher strain (Sriapai et al., 2012: Pudewills et al., 1995: Cristescu and Hunsche, 1996: Hamami et al., 1996: Charpentier, 1984). The results obtained have will be used to calibrate the creep and elastic parameters of the constitutive model presented in the next chapter.

CHAPTER IV

CREEP PARAMETERS CALIBRATION

4.1 Introduction

The purpose of this chapter is to describe the calibration results of salt property creep parameters. The data used in the calibration are obtained from the uniaxial creep tests under temperatures of 0 and 30 Celsius.

4.2 Exponential Law

To assess the effect of the time-dependent properties on salt for creep tests, simple exponential creep model is used to describe behavior of the salt. The calibration uses regression analysis method. The exponential law presents the creep behavior of salt as a function of constant stress, constant temperatures and time using following exponential relation (Senseny, 1983)

$$\varepsilon(t) = B'\sigma^{m} t^{n} \exp\left(\frac{-\lambda}{T}\right) \tag{4.1}$$

The time-dependent deformation of salt can be divided into two parts: elastic strains (linear and recoverable strain) and plastic creep strains (time-dependent and nonrecoverable strain) in terms of the octahedral shear stress (τ_{oct})

$$\gamma_{oct}(t) = \frac{\tau_{oct}}{G} + \alpha\tau_{oct}^{\beta} t^{\gamma} \exp\left(\frac{-\lambda}{T}\right) : \text{Transient phase} \tag{4.2}$$

$$G = AT + B \tag{4.3}$$

The octahedral shear strain rate of salt in steady state phase can be differential Eqs. (4.2) as a function of time:

$$\dot{\gamma}_{oct}(t) = \kappa\tau_{out}^{\beta} t^{\gamma-1} \exp\left(\frac{-\lambda}{T}\right) : \text{Steady state phase} \tag{4.4}$$

where γ_{oct} is the octahedral shear strains, is the octahedral shear strains rate, τ_{oct} are the octahedral shear stress, G is shear modulus as function of temperatures (Sriapai et al. 2012), T is temperature (Kelvin), t is time, α is stress constant, β is stress exponent, γ is time exponent and λ, κ are constant creep parameters. The creep parameters are calibrated by SPSS program in terms of the octahedral shear stress (τ_{oct}) for the transient creep phase and the steady-state phase as follows Equations. (4.2) – (4.4). Figures 4.1 and 4.2 show the calibration of the transient creep phase by using equation (4.2) and steady-state creep phase by using equation (4.4) under low and ambient temperatures. The parameters of transient and steady-state creep phase are summarized in Table 4.1. The coefficients of correlation (R^2) can be calculated as 0.967 for transient phase and 0.964 for steady-state phase.

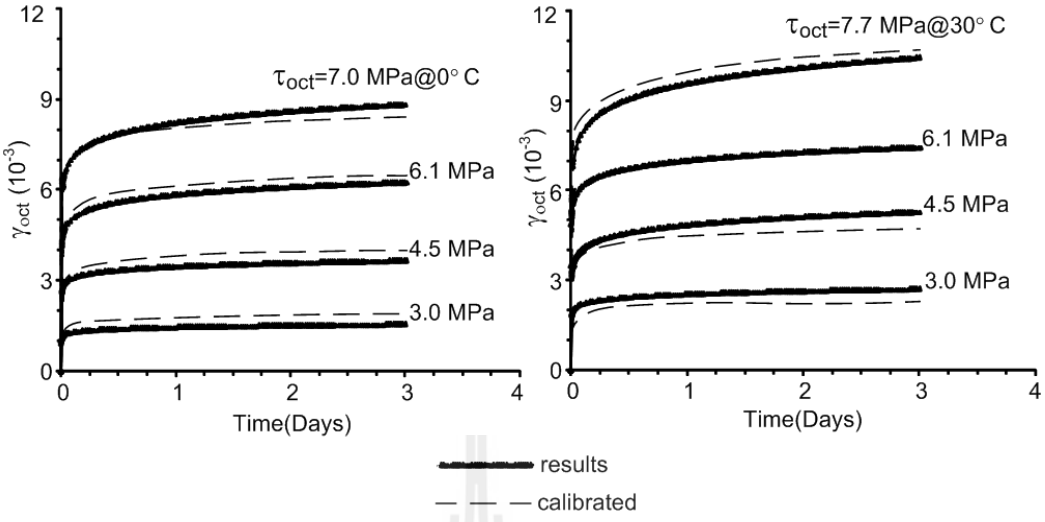

Figure 4.1 Octahedral shear strain-time curves for transient creep phase during the first 3 days.

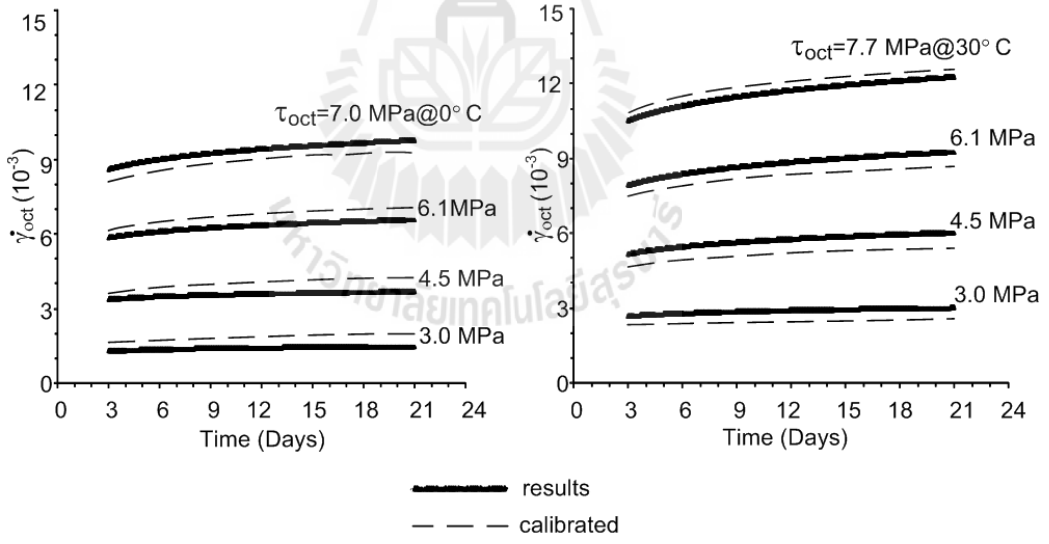

Figure 4.2 Octahedral shear strain-time curves for steady-state creep phase.

Table 4.1 Creep parameters.

Creep parameters	**Transient creep phase**	**Steady-state creep phase**
α	1.238	-
κ	-	1.890
β	1.581	1.620
γ	0.063	0.072
λ	347.267	493.468
A	-21.5×10^{-3}(Sriapai et al., 2012)	-
B	16.200 (Sriapai et al., 2012)	-
R^2	**0.967**	**0.964**

4.3 Discussions

The time-dependent parameters from the uniaxial creep tests results are compared with ambient and low temperatures. The creep parameters are the transient phase and steady state phase used to the simulation model of salt cavern in next chapter. The test results fit well to the proposed exponential creep law, as suggested by the high value of the correlation coefficients.

CHAPTER V

COMPUTER SIMULATIONS

5.1 Introduction

This chapter describes the results of finite difference analyses using FLAC (Itasca, 1992) to demonstrate the impact of low temperature on the salt behavior around a CO_2 storage cavern. The time-dependent parameters calibrated from the uniaxial creep tests are used in the computer simulation.

5.2 Numerical simulations

A finite element analysis with the creep model discussed in the previous chapter is performed to demonstrate the impact of low temperatures on the salt behavior around a CO_2 storage cavern. For this demonstration, the cavern is taken as an upright cylinder with a diameter of 50 m and spherical cavern with diameter of 50 m. The top of the cavern is assumed at 500 m depth. The Norton power law (Norton, 1929) is commonly used to model the creep behavior of salt. The standard form of this law is:

$$\dot{\varepsilon}_{cr} = A\sigma^{-n} \tag{5.1}$$

where $\dot{\varepsilon}_{cr}$ is the creep rate, A and n are material properties, σ^{-} is the deviatoric part of the deviatoric stresses. This study uses this equation to simulate and analyze the salt deformation in FLAC program. The analysis is made in axis symmetry.

The power model under isothermal condition is assumed. It is assumed that no nearby underground structure within 500 m radius for the cylinder cavern and 325 m radius for the spherical cavern. The top and bottom of the cavern are assumed at 500 m and 1000 m depth for cylindrical cavern. The spherical cavern is assumed from at 500 m to 1050 m for top and bottom of the cavern. Figures 5.1 and 5.2 shows the finite difference mesh constructed to simulate a CO_2 storage cavern for the cylindrical and spherical caverns.

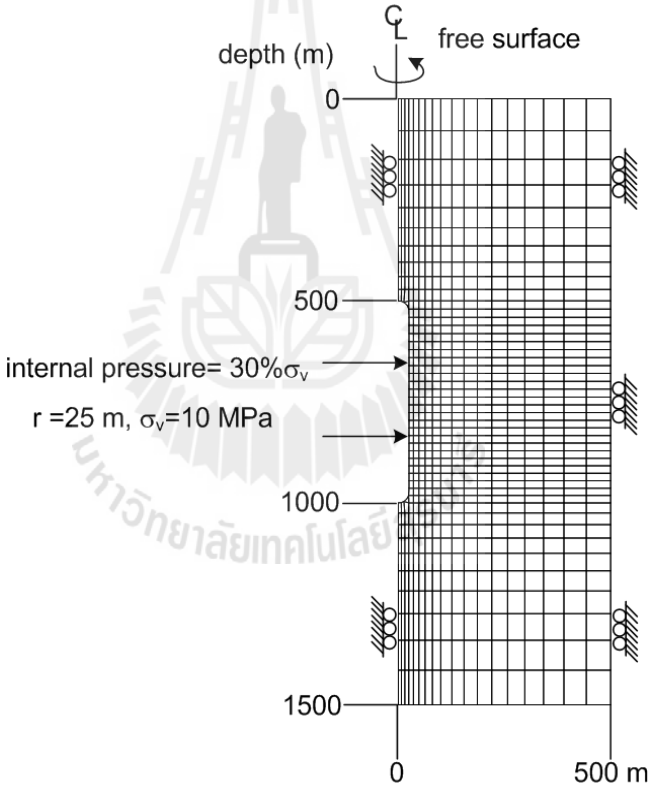

Figure 5.1 Finite difference mesh constructed to simulate CO_2 storage cylindrical cavern in the Maha Sarakham salt.

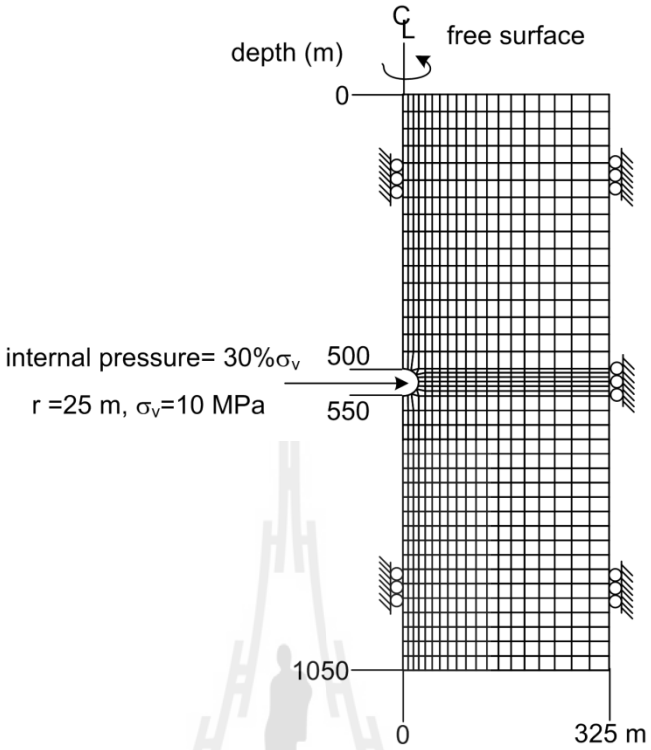

Figure 5.2 Finite difference mesh constructed to simulate CO_2 storage spherical cavern in the Maha Sarakham salt.

The both storage cavern models are subject to the internal pressure of 30% (3 MPa) and of the in-situ stress at the cavern top. The internal pressures are assumed to be uniform on the cavern boundary. Sriapai et al. (2012) determine the temperature effect on salt strength while is implicitly considered by incorporating empirical relations between the elastic parameters and temperatures of the tested specimens. The proposed criterion agrees well with the test results obtained under temperatures ranging from 273 to 467 Kelvin. The correlations are obtained when they are fitted with the following linear equations:

$$G(\text{GPa}) = -0.0215T + 16.2 \tag{5.2}$$

$$E(GPa) = -0.06T + 42.7 \quad (5.3)$$

$$K(GPa) = -0.0254T + 35.6 \quad (5.4)$$

$$\nu = (7 \times 10^{-6})T + 0.33 \quad (5.5)$$

$$c(MPa) = -0.0135T + 12.5 \quad (5.6)$$

$$\phi(degree) = -0.0426T + 57.9 \quad (5.7)$$

Two sets of property parameters are used in the simulation. The power model of property parameters are used in the simulation, which are calibrated from the uniaxial creep tests in Table 5.1 under temperatures of 0 and 30 Celsius.

Table 5.1 Material properties used in FLAC simulations.

Salts property	**Low tem. (0°C)**	**Room tem. (30°C)**	**Reference**
Elastic Modulus, E (GPa)	26.32	24.52	Sriapai et al., 2012
Shear Modulus, G (GPa)	10.33	9.68	
Bulk Modulus, K (GPa)	28.93	28.20	
Friction angle, ϕ (Degrees)	46.27	44.99	
Cohesion, c (MPa)	8.81	8.41	
Poisson's ratio, ν	0.35	0.35	
Tensile strength (MPa)	1.5	1.5	Phueakphum and Fuenkajorn (2010)
Thermal conductivity, k (W/m·K)	5.8	5.8	Phueakphum and Fuenkajorn (2011)
Specific heat, C (MJ/m^3)	1.83	1.83	
Thermal expansion (K^{-1})	40	40	
Density, ρ (g/cc)	2.2	2.2	
Internal pressure (MPa)	3	3	

5.3 Results

The FLAC results indicate the cavern closure simulated using parameters calibrated from the low and ambient temperatures are different. Two caverns are taken as with a diameter of 50 m. The factor of safety of two caverns in both temperatures conditions are shown in Table 5.2. The results also show the distributions of the maximum stress, minimum stress, stress deviations and displacement vectors under both temperatures and both cavern shapes (Figures 5.3 through 5.8).

5.4 Discussions

The FLAC simulations determine that the cavern closure simulated using parameters calibrated from the uniaxial creep test results. The factor of safety of salt cavern decreases as temperature increases. The spherical cavern shows higher the factor of safety than the cylindrical cavern. The stress-strain distribution (stress deviation, maximum stress, minimum stress, displacement vector) of the cylindrical cavern shows higher values than those of the spherical cavern. The deformation of cylindrical cavern are higher than those the spherical cavern. The results of both salt cavern shapes show salt cavern deformation in terms of diameter closure where increase with temperatures, as shows in Figures 5.9 and 5.10. The shows the diameter closure at depth of 500 m as function of time for both cavern shapes. This suggests that determination of the cavern closure using the parameters calibrated from the conventional creep testing may not conservative.

Table 5.2 Factor of safety of salt cavern calculated from FLAC simulations.

Cavern shape	Factor of Safety	
	Low Temperature. (0°C)	**Ambient Temperature. (30°C)**
Cylindrical shape	4.46	4.44
Spherical shape	5.53	5.50

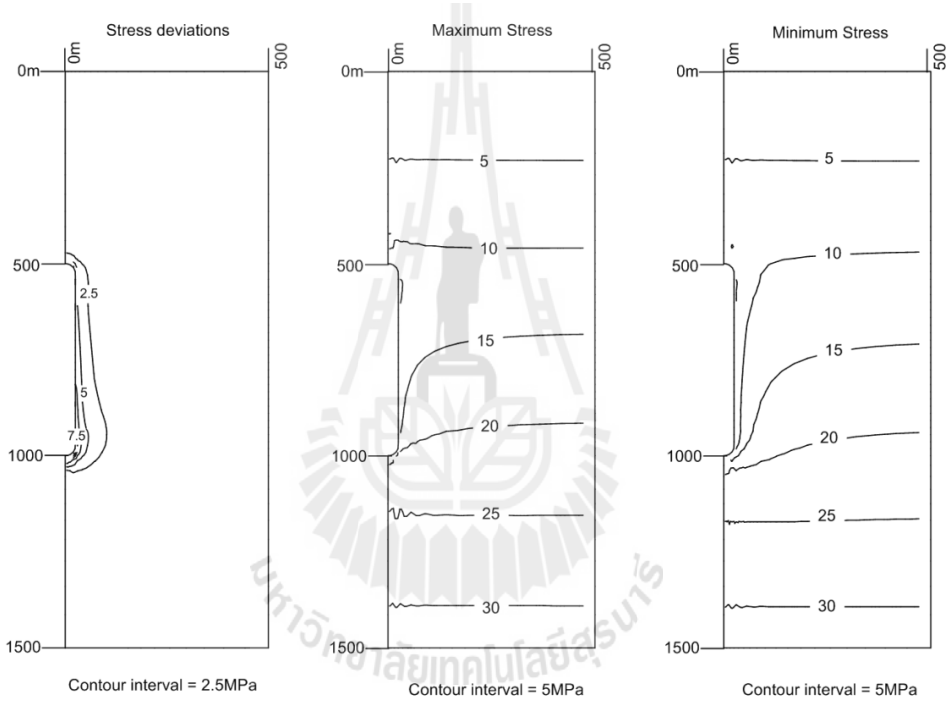

Figure 5.3 Stress distributions around salt cavern for cylindrical shape under low temperature.

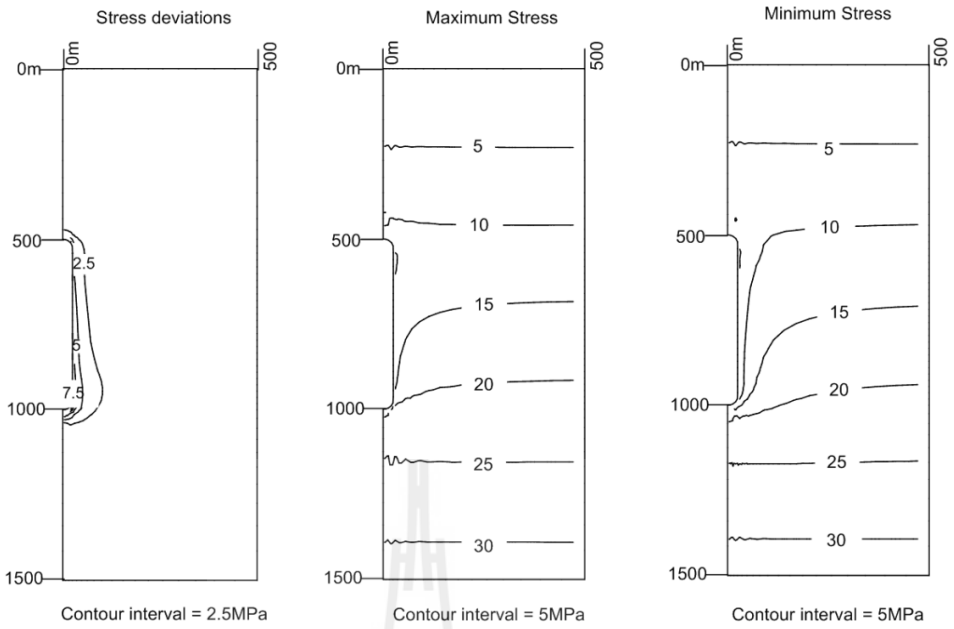

Figure 5.4 Stress distributions around salt cavern for cylindrical shape under ambient temperature.

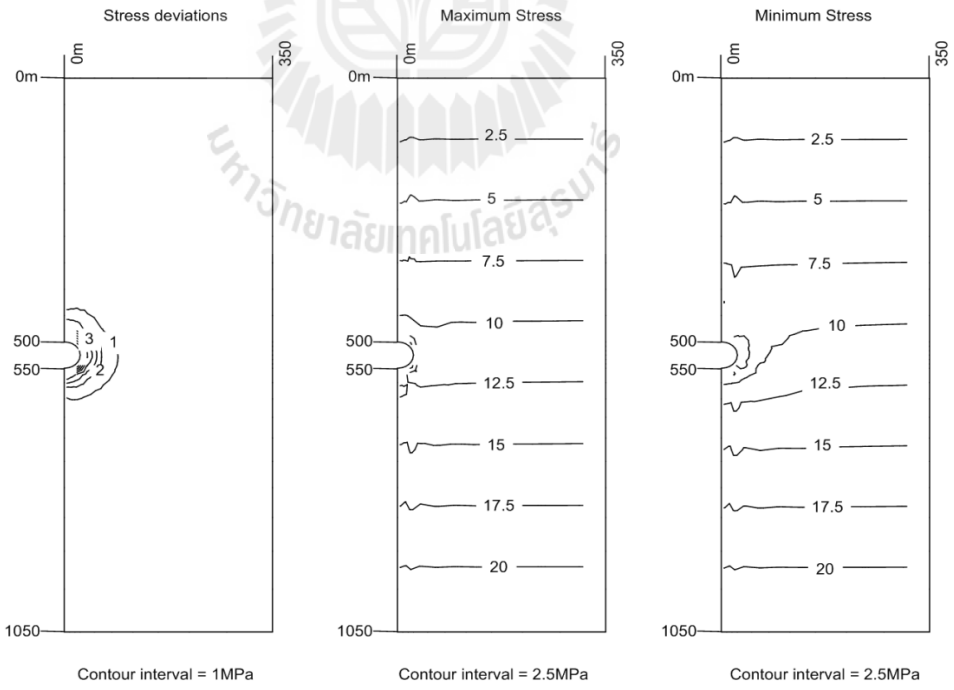

Figure 5.5 Stress distributions around salt cavern for spherical shape under low temperature.

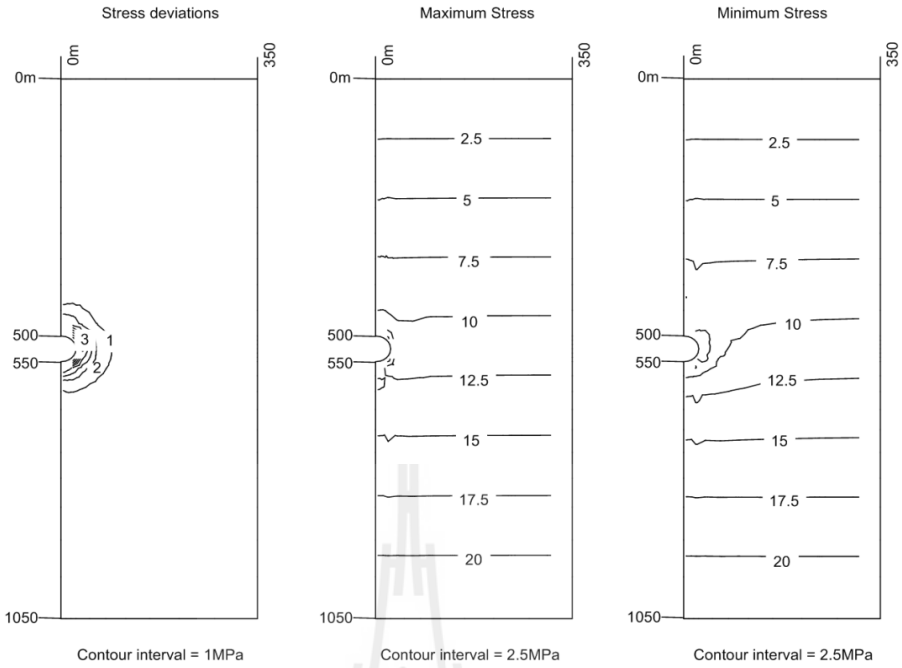

Figure 5.6 Stress distributions around salt cavern for spherical shape under ambient temperature.

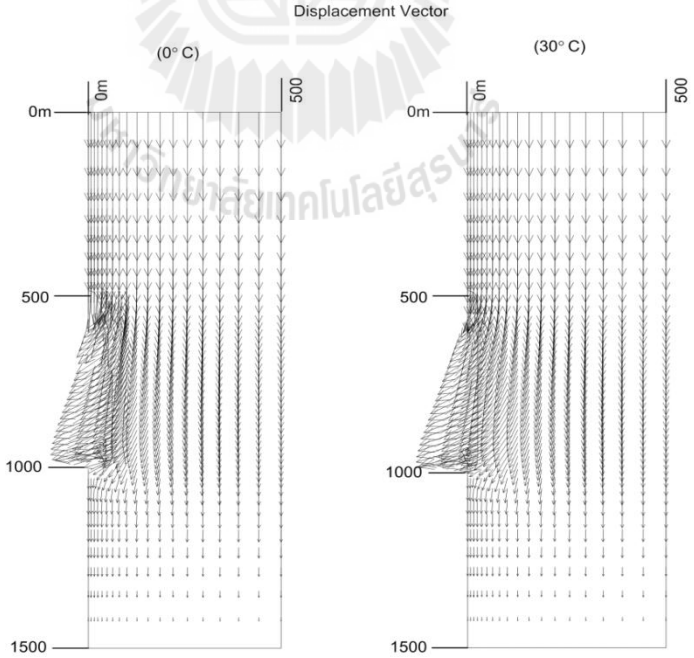

Figure 5.7 Displacement vectors around salt cavern for cylindrical shape under low (left) and ambient (right) temperatures.

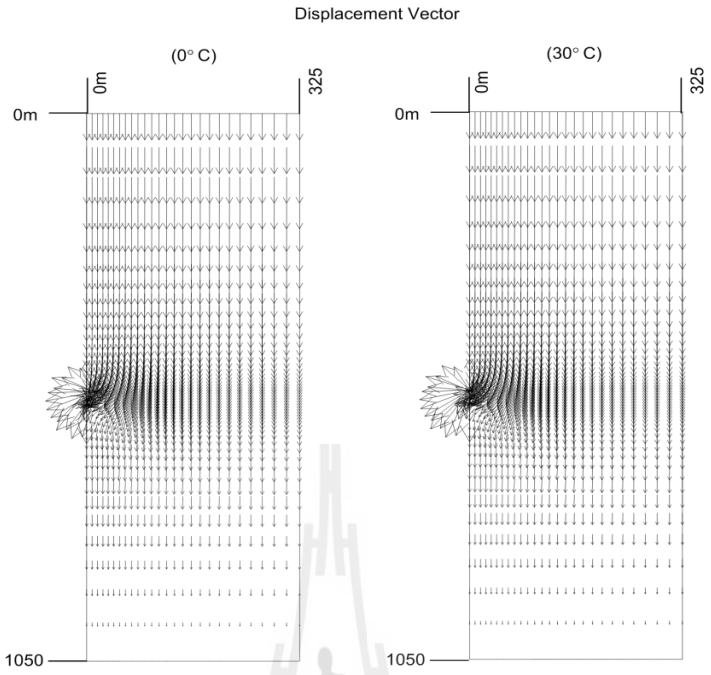

Figure 5.8 Displacement vectors around salt cavern for spherical shape under low (left) and ambient (right) temperatures.

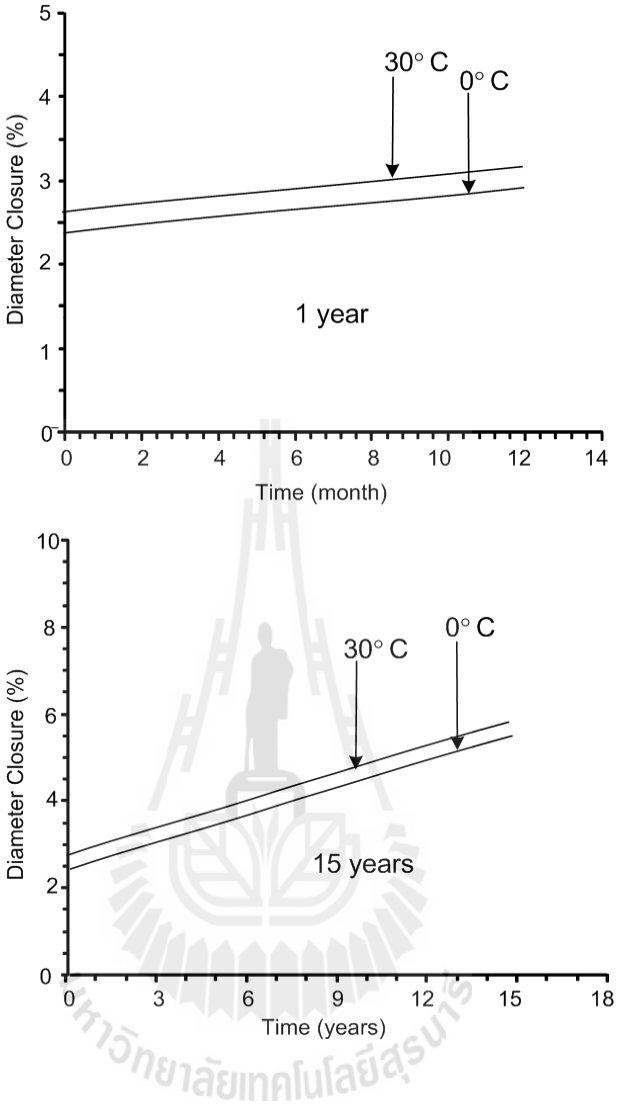

Figure 5.9 Cavern closure using parameters from the uniaxial creep test under both temperatures as function of time for cylindrical shape cavern.

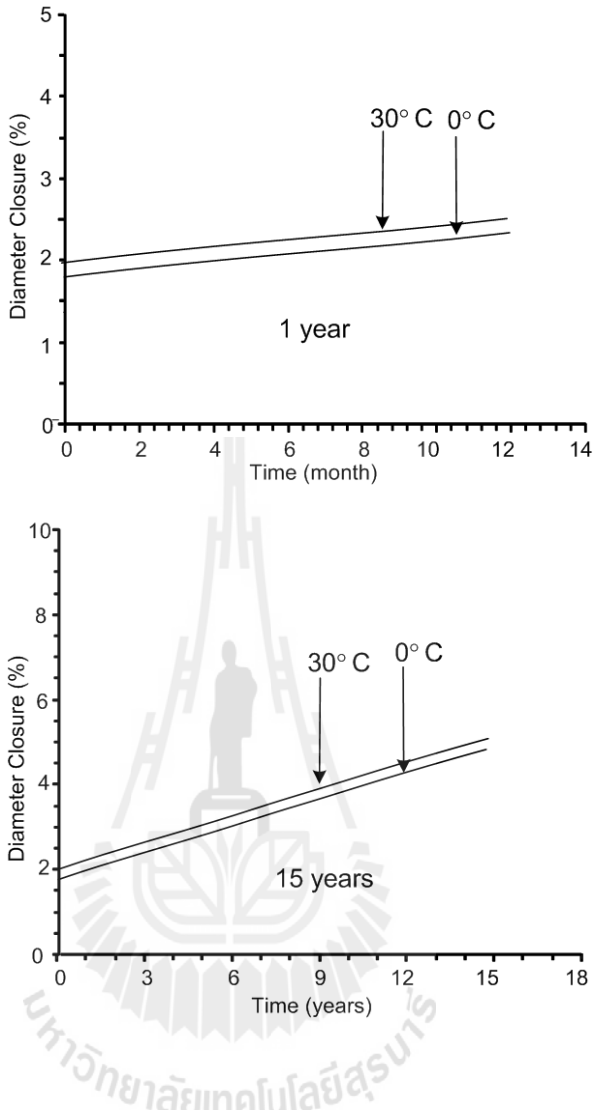

Figure 5.10 Cavern closure using parameters from the uniaxial creep test under both temperatures as function of time for spherical shape cavern.

CHAPTER VI

DISCUSSIONS, CONCLUSIONS AND RECOMMENDATIONS FOR FUTURE STUDIES

6.1 Discussions and conclusions

The objective of this study is to determine the effect of low temperature on the time-dependent behavior of rock salt. Uniaxial creep tests have been performed to determine the effect of low temperatures on the time-dependent deformation of the Maha Sarakham rock salt. The salt specimens are prepared to have nominal dimensions of 10 cm in diameter and 25 cm in length. The constant axial stresses are applied using consolidation load frames. The constant axial stresses are 6.5, 9.6, 13.0, 14.8 and 16.0 MPa (about 20% to 50% of the uniaxial compressive strength). The testing temperatures are 0 and 30 Celsius. The tests methods and calculation follow the ASTM (D7070-08) standard practice. The test duration is 21 days. The exponential creep law is used to describe the time-dependent deformations of the salt specimens. The test results indicate that the creep deformation increases with the temperatures. The transient creep increases with time and tends to be constant at steady-state creep phase. Salt creep under the low temperature is lower than that under the ambient temperature. The exponential creep law agrees well with the test results in terms of the octahedral shear strains as a function of time.

The closure of CO_2 storage cavern is simulated using parameters calibrated from the uniaxial creep test results. The stress and strain distributions around the storage cavern are determined for spherical and cylindrical caverns. The factor of safety of salt caverns decreases as temperature increases. The creep deformations of both salt cavern shapes show salt cavern deformation in terms of diameter closure. The closure is 1.38 m for cylindrical cavern and 1.18 m for spherical cavern under low temperature. The closure is 1.48 m for cylindrical cavern and 1.25 m for spherical cavern under ambient temperature.

6.2 Recommendations for future studies

The uncertainties and adequacies of the research investigation and results discussed above lead to the recommendations for further studies. The test specimens here are relatively small. Testing on larger specimens is desirable to confirm the research findings. Testing time should be increased to obtain a longer trend of the strain-time curves in the creep, hence revealing clearer effects of low temperatures. Temperature test range should be broader to higher or to lower. The constitutive law used in this study is the exponential model and may not adequately describe the salt behavior. Other constitutive laws, such as liner visco-plastic and Burger's laws may be needed to describe the salt behavior. The effect of cyclic thermal and mechanical loading should be assessed.

REFERENCES

ASTM D4543. Standard practice for preparing rock core specimens and determining dimensional and shape tolerances. In **Annual Book of ASTM Standards** (Vol. 04.08). Philadelphia: American Society for Testing and Materials.

ASTM D7070. Creep of rock core under constant stress and temperature. In **Annual Book of ASTM standards** (Vol. 04.08). ASTM International: West Conshohocken, PA.

Bachu, S. and Dusseault, M. B. (2005). Underground injection of carbon dioxide in salt beds. **Developments in Water Science**. 52: 637-648.

Berest, P., Brouard, B. and Durup, J. G. (2000). Shut-in pressure test: Case studies. In **Proceedings Solution Mining Research Institute 2000 Fall Technical Meeting** San Antonio, TX.

Bradley, R. A., Watts, E. C. and Williams, E. R. (1991). Limitting netv greenhouse gas emission in the U.S. **Report to the US congress**. Vol. 1.

Charpentier, J-P. (1984). Creep of rock salt elevated temperature. In **Proceedings of the Second Conference on the Mechanics Behavior of Salt** (pp. 131-136). Clausthal, Germany: Trans Tech Publications.

Coleman, B. D. and Noll, W. (1961). Foundations of linear viscoelasticity. **Reviews of Modern Physics** 33(2): 239-249.

Cristescu, N. and Hunsche, U. (1996). A comprehensive constitutive equation for rock salt determination and application. In **Proceedings of the Third Conference on the Mechanical Behavior of Salt** (pp. 191-205). Clausthal-Zellerfeld, Germany: Trans Tech Publications.

Durham, W. B., Olgaard, D. L., Urai, J. L. and Schoenherr, J. (2008). Creep of rock salt at low temperatures. In **Proceedings of the 42nd U.S. Rock Mechanics Symposium** (pp. 387-392). San Francisco, CA.

Dusseault, M. B. and Fordham, C. J. (1993). Time-dependent behavior of rocks. **Comprehensive Rock Engineering Principles, Practice and Project: Rock Testing and Site Characterization.** (Vol. 3, pp. 119-149). London, Pergamon.

Dwivedi, R. D., Goel, R. K., Prasada, V. V. R. and Sinhab, A. (2008). Thermo-mechanical properties of Indian and other granites. **International Journal of Rock Mechanics and Mining Sciences** 45: 303-315.

Farmer, I. W. (1983). **Engineering behavior of rock.** 2nd Edition, Chapman and Hall, New York.

Fuenkajorn, K. and Daemen, J. J. K. (1988). **Boreholes closure in salt**. Technical Report Prepared for The U.S. Nuclear Regulatory Commission. Report No. NUREG/CR-5243 RW. University of Arizona.

Gnirk, P. E. and Johnson, R. E. (1964). The deformation behavior of a circular mine shaft situated in a viscoelastic medium under hydrostatic stress. In **Proceedings of the 6th U.S. Symposium on rock Mechanics** (pp. 233-259). University of Missouri, Rolla.

Hamami, M., Tijani, S. M. and Vouille, G. (1996). A methodology for the identification of rock salt behavior using multi-steps creep tests. In **Proceedings of the Third Conference on the Mechanical Behavior of Salt** (pp. 53-166). Geosciences and Natural Resource: Germany.

Inada, Y., Kinoshita, N., Ebisawa, A. and Gomi, S. (1997). Strength and deformation characteristics of rocks after undergoing thermal hysteresis of high and low temperatures. **International Journal of Rock Mechanics and Mining Sciences** 34 (3-4): 688-702.

Itasca. 1992. **User Manual for FLAC-Fast Langrangian Analysis of Continua, Version 4.0.** Itasca Consulting Group Inc. Minneapolis, Minnesota.

Jaeger, J. C., Cook, N. G. W., and Zimmerman, R. W. (2007). **Fundamentals of Rock Mechanics**. Chapman and Hall, London, 474 p.

Jandakaew, M. (2007). Stress-path dependency of rock salt. In **Proceedings of First Thailand Symposium on Rock Mechanics** (pp. 171-188). September, 13-14, Greenery Resort, Khao Yai, Nakhon Ratchasima, Suranaree University of Technology,

Jeremic, M. L. (1994). **Rock mechanics in salt mining**. Rotherdam: A. A. Balkema. pp. 530.

Knowles, M. K., Borns, D., Fredrich, J., Holcomb, D., Price, R. and Zeuch, D. (1998). Testing the disturbed zone around a rigid inclusion in salt. In **Proceedings of the Fourth Conference on the Mechanical Behavior of Salt** (pp. 175-188). Clausthal, Germany: Trans Tech Publications.

Langer, M. (1984). The Rheological behavior of rock salt, Mechanical behavior of salt I. In **Proceedings of the First Conference on the Mechanical Behavior of Salt** (pp. 201-240). Clausthal-Zellerfeld, Germany: Trans Tech Publications.

Norton, F. H. (1929). **Creep of steel at high temperatures**. New York: McGraw-Hill Book Company

Phueakphum, D. and Fuenkajorn, K. (2010). Effects of cyclic loading on mechanical properties of Maha Sarakham salt. **Engineering Geology** 112: 43-52.

Phueakphum, D. and Fuenkajorn, K. (2011). Laboratory test model for solar energy storage in rock fills. In **Proceedings of Third Thailand Symposium on Rock Mechanics** (pp. 171-188). March, 12-13, Springfield Sea Resort and Spa, Cha-Am Beach, Suranaree University of Technology,

Pudewills, A. (1995). **Thermal Simulation of Drift Emplacement**: Temperature Analyses.Topical Report, Forschungszentrum Karlsruhe.

Pudewills, A. and DrostePapp, J. (2003). Numerical modeling of the thermomechanical behavior of a large-scale underground experiment. **Computers & Structures**. 81: 911-918.

Senseny, P. E. (1983). **Review of constitutive laws used to describe the creep of salt**. Battelle Memorial Institute. Columbus.

Sriapai, T., Walsri, C. and Fuenkajorn, K. (2012). Effects of temperature on compressive and tensile strengths of salt. **ScienceAsia**. 38: 166-174.

Tek, M. R. (1989). **Underground storage of natural gas.** theory and practice. Applied Sciences, Kluwer: Boston. Vol. 171.

Yanan, G., Feng, G., Zhizhen, Z. and Tao, Z. (2010). Visco – elastic model of deep underground rock affect by temperature and humidty. **Mining Science and Technology** 20: 183-187.

APPENDIX A

TECTHICAL PUBLICATION

TECHNICAL PUBLICATION

Khathipphathee, T., and Fuenkajorn, K., (2013). **Performance assessment of Maha Sarakham salt for CO2 storage.** In Proceeding of Fourth Thai Rock Mechanics Symposium, Nakhon Ratchasima Thailand, 24-25 January 2013.

Rock Mechanics, Fuenkajorn & Phien-wej (eds) © 2013

Performance assessment of Maha Sarakham salt for CO_2 storage

T. Khathipphathee & K. Fuenkajorn
Geomechanics Research Unit, Suranaree University of Technology, Thailand

Keywords: Sequestration, salt cavern, creep, carbon emission

ABSTRACT: Uniaxial creep tests have been performed to assess the effect of low temperatures on the time-dependent deformation of the Maha Sarakham rock salt. The salt specimens are prepared to have nominal dimensions of 10 cm in diameter and 25 cm in length. The constant axial stresses are applied using consolidation load frames. The constant axial stresses are 6.5, 9.6, 13.0, 14.8 and 16.0 MPa (about 20% to 50% of the uniaxial compressive strength). The testing temperatures are 273 and 303 K. The tests methods and calculation follow the ASTM (D7070-08) standard practices. The test duration is 21 days. The Exponential creep law is used to describe the time-dependent deformations of the salt specimens. The test results indicate that the creep deformation increases with the temperatures. The test results show that the transient creep under low temperature decreases with time and tends to be constant at steady-state creep phase.

1 INTRODUCTION

Geological sequestration of CO_2 is a mitigation option for significantly reducing CO_2 emissions into the atmosphere that is immediately available and technologically feasible. The technology has already been developed and applied for underground storage of petroleum, natural gas and compressed air (e.g., Tek, 1989; Bradley et al., 1991) or for salt mining. Sequestration of CO_2 in salt caverns differs from natural gas storage in terms of time scale, as a result the long-term behavior of the salt cavern needs investigating in terms of permanency and safety of the operation. Storage of fluids in crustal caverns often requires cryogenic conditions to keep such fluids in a condensed state and maximize storage capacity (Durham et al., 2008).

The objective of this study is to determine experimentally the effects of low temperatures on the time-dependent deformation of the Maha Sarakham rock salt. The uniaxial creep test is performed under isothermal condition at 273 and 303 K (0 and 30°C). A constitutive relation between the mechanical loadings and the creep deformation of the salt under varied temperatures will be derived.

2 SALT SPECIMENS

The tested specimens are prepared from 100 mm diameter salt core drilled from depths ranging between 70 m to 170 m by Asean Potash Mining Co. in the northeast of Thailand. The salt cores belong to the Middle Salt member of the Maha Sarakham formation. The origin and geological description of the Maha Sarakham salt basin are provided by Warren (1999). The drilled cores are dry-cut to obtain cylindrical shaped specimens with nominal dimensions of 10 cm in diameter and 25 cm in length (L/D = 2.5). Over 10 specimens are prepared (Figure 1). After preparation, the specimens are labeled and wrapped with plastic film. Preparation of these samples follows as much as practical the ASTM (D4543-08) standard practices. The average density is 2.2±0.2 g/cm^3. Phueakphum and Fuenkajorn (2010) determine the mechanical properties of the same salt under uniaxial conditions, and report that the uniaxial compressive strength, internal friction angle and cohesion of the salt are 34.7±2.2 MPa, 39° and 1.5±0.4 MPa respectively. The elastic modulus and Poisson's ratio are 21.5±2.6 GPa and 0.40±0.4.

3 UNIAXIAL CREEP TESTS

3.1 Consolidation Load Frame

A consolidation load frame has been used to apply constant axial stress to cylindrical rock specimens. A cooling system is fabricated to test the salt cylindrical sample while loading (Figure 2). It can cool the salt specimens down to 273K. Figure 3 shows the room temperature testing. The consolidation load frame has been used in this study because the cantilever beams with pre-calibrated dead weight can apply a truly constant axial stress to specimen.

3.2 Test Method

The uniaxial creep test procedure and apparatus follow the ASTM (D7070-08) standard practice as much as practical. The salt specimens are installed into the consolidation load frame to provide constant axial stresses. The axial load is pre-calibrated with a proving ring to obtain an equivalent axial stress on the specimens. The applied constant axial stresses are 6.5, 9.6, 13.0, 14.8 and 16.0 MPa (about 20% to 50% of the uniaxial compressive strength). The specimen deformations are monitored along the three principal axes for up to 21 days. During the test, the axial and lateral deformations are monitored. The specimen deformations are monitored using four dial gages with high precision (±0.01 mm).

3.3 Results

Figures 4 and 5 show the axial and lateral strain-time curves of salt specimens with constant axial stresses range from 6.5 to 16 MPa under low and ambient temperatures. Each salt specimen shows instantaneous deformation, transient creep phase and steady-state creep phase.

The octahedral shear strains (γ_{oct}) and mean strain (ε_m) can be determined by (Jaeger et al., 2007):

$$\gamma_{oct} = 1/3[((\varepsilon_1 - \varepsilon_2)^2 + (\varepsilon_1 - \varepsilon_3)^2 + (\varepsilon_2 - \varepsilon_3)^2)]^{1/2} \quad (1)$$

Rock Mechanics, Fuenkajorn & Phien-wej (eds) © 2013

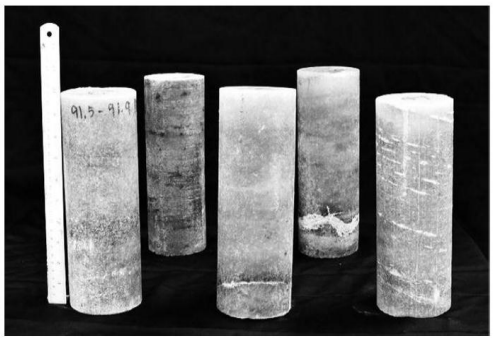

Figure 1. Some cylindrical salt specimens prepared for the uniaxial creep testing.

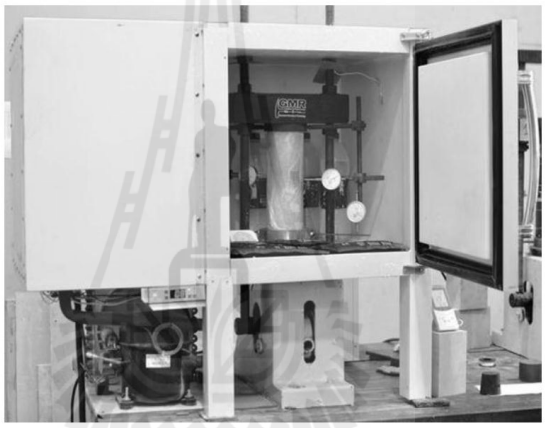

Figure 2. Salt specimen placed in the consolidation load frame and inside the cooling system for low temperature test at 273 K.

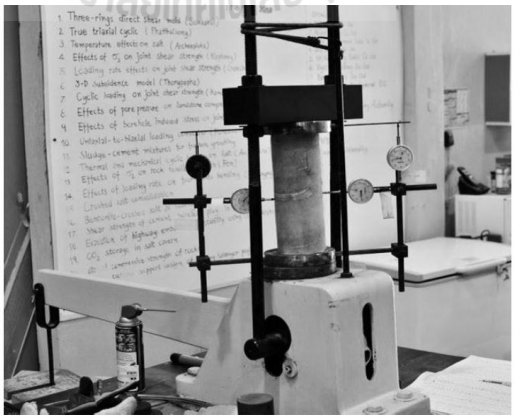

Figure 3. Salt specimen placed in consolidations loading frame under room temperatures (about 303 K).

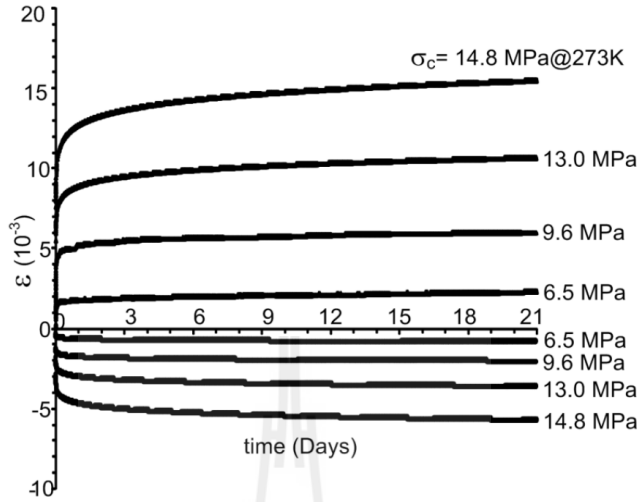

Figure 4. Axial and lateral strain-time curves for under 273 K.

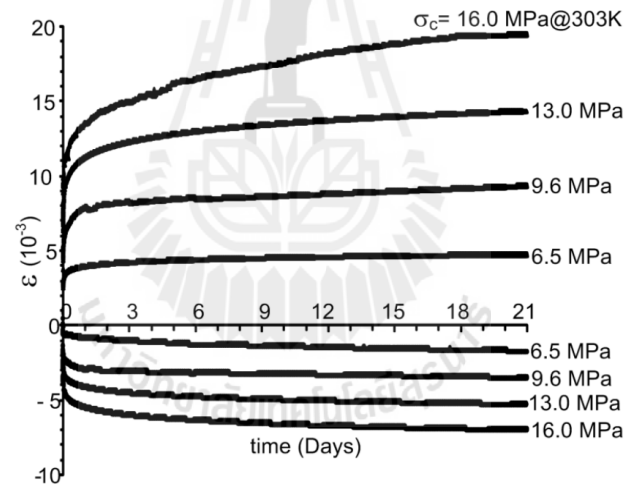

Figure 5. Axial and lateral strain-time curve for under 303 K.

$$\varepsilon_m = \frac{1}{3}(\varepsilon_1 + \varepsilon_2 + \varepsilon_3) \quad (2)$$

where γ_{oct} is the octahedral shear strains, ε_m is the mean strains, ε_1, ε_2 and ε_3 are the major, intermediate and minor principal strains measured during the tests ($\varepsilon_{axial} = \varepsilon_1$). Here the intermediate and minor principal strains are equal ($\varepsilon_{lateral} = \varepsilon_2 = \varepsilon_3$).

The octahedral shear strains and the means strains under low and ambient temperature are plotted as a function of time in Figures 6 and 7 respectively. The test results show the transient creep phase of low temperature decreases with time and tend to be constant in steady-state creep phase. Higher creep strains are observed from the room temperatures test results.

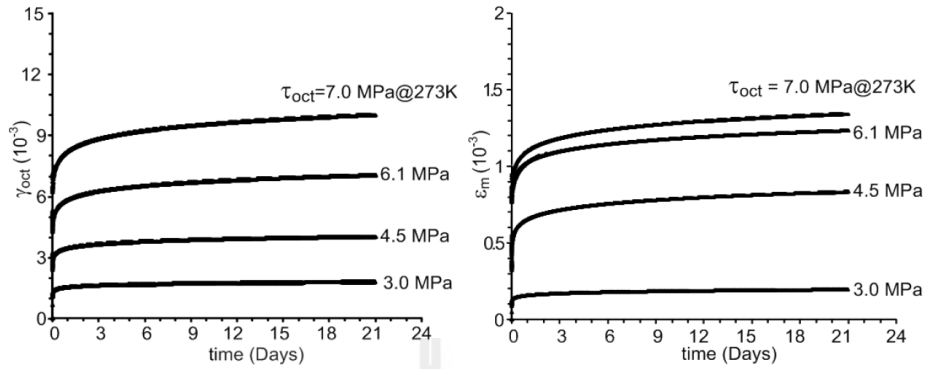

Figure 6. Octahedral shear strain-time curves (left) and mean strain-time curves (right) under at 273 K.

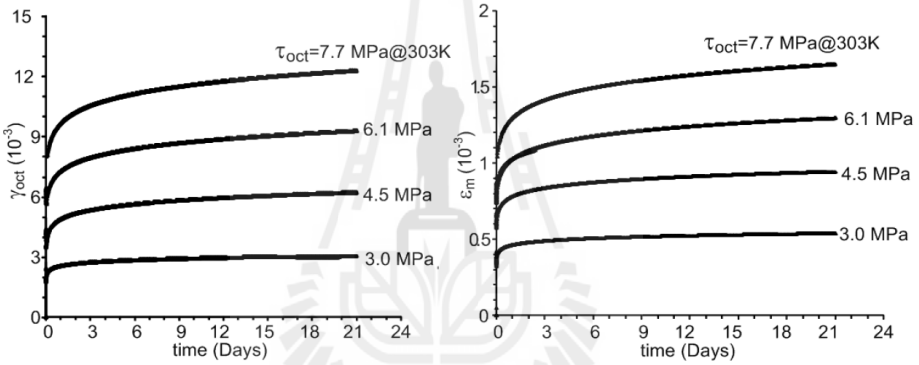

Figure 7. Octahedral shear strain-time curves (left) and mean strain-time curves (right) under 303 K.

4 EXPONENTIAL LAW

Exponential law is applied to describe the time-dependent behavior of salt. Generally, empirical constitutive model are developed by linking the creep strain to stress and temperature. The exponential law presents the creep behavior of salt as a function of constant stress, constant temperatures in function of time (Senseny, 1983).

To assess the effect of the time-dependent properties on salt for creep tests, simple exponential creep model is used to describe behavior of the salt. The salt properties calibration of creep tests uses regression analysis methods. The exponential law presents the creep behavior of salt as a function of constant stress, constant temperatures and time using following exponential relation:

$$\varepsilon(t) = B'\sigma^{m}t^{n}\exp\left(\frac{-\lambda}{T}\right) \quad (3)$$

The creep parameters are calibrated by SPSS program in terms of the octahedral shear stress (τ_{oct}) for the transient creep phase and the steady-state phase as follows:

$$\gamma_{oct}(t) = \frac{\tau_{oct}}{G} + \alpha\tau_{oct}^{\beta} t^{\gamma} \exp\left(\frac{-\lambda}{T}\right); \qquad [G = AT + B] \tag{4}$$

$$\dot{\gamma}_{oct}(t) = \kappa t^{\gamma-1} \exp\left(\frac{-\lambda}{T}\right) \tag{5}$$

where γ_{oct} is the octahedral shear strains, $\dot{\gamma}_{oct}$ is the octahedral shear strains rate, τ_{oct} are the octahedral shear stress, G is shear modulus, T is temperature (Kelvin), t is time, α is stress constant, β is stress exponent, γ is time exponent and λ, κ are constant creep parameters. Figures 8 and 9 show the calibration of the transient creep phase by using equation (4) and steady-state creep phase by using equation (5) under low and ambient temperatures. The parameters of transient and steady-state creep phase are summarized in Table 1. The coefficients of correlation (R^2) can be calculated as 0.967 for transient phase and 0.964 for steady-state phase.

The creep parameters (Table 1) calibrated from uniaxial creep test are used to determine the effect of low temperatures on time-dependent closure of a salt cavern. The solution of circular hole in infinite plate of viscoplastic materials is applied to analyze with effect of temperatures. The radial strains can be divided into two parts are elastic and plastic creep strains.

$$\varepsilon_r = \varepsilon_r^e + \varepsilon_r^c \tag{6}$$

where ε_r is the radial strains, ε_r^e is elastic radial strains, ε_r^c is plastic radial (or creep) strains, with can be calculated from radial stresses (Obert and Duvall, 1967)

$$\varepsilon_r^e = \frac{1}{E}\left\{(1-\nu^2)\sigma_r - \nu(1+\nu)\sigma_\theta\right\} \tag{7}$$

The exponential law (Eqs. 3 and 4) is used to describe creep behavior or plastic radial strains of salt.

$$\varepsilon_r^c = \frac{3}{2}\alpha(\sigma^*)^{(\beta-1)} t^{\gamma} \exp\left(\frac{-\lambda}{T}\right) \cdot S_r \tag{8}$$

$$\sigma^* = \frac{1}{\sqrt{2}}\left\{(\sigma_r - \sigma_\theta)^2 + (\sigma_\theta - \sigma_z)^2 + (\sigma_z + \sigma_r)^2\right\}^{\frac{1}{2}} \tag{9}$$

$$S_r = \sigma_r - (\sigma_r + \sigma_\theta + \sigma_z)/3 \tag{10}$$

$$\sigma_r = P_o\left(1 - \frac{R^2}{r^2}\right) + \frac{P_i R^2}{r^2}; \ \sigma_r = P_o\left(1 + \frac{R^2}{r^2}\right) - \frac{P_i R^2}{r^2}; \ \sigma_z = \nu(\sigma_r + \sigma_\theta) \tag{11}$$

Substitute Eqs. (7) through (11) into (6) we obtain:

$$\varepsilon_r = \frac{1}{E}\left\{(1-\nu^2)\sigma_r - \nu(1+\nu)\sigma_\theta\right\} + \frac{3}{2}\alpha(\sigma^*)^{(\beta-1)} t^{\gamma} \exp\left(\frac{-\lambda}{T}\right) \cdot S_r \tag{12}$$

Rock Mechanics, Fuenkajorn & Phien-wej (eds) © 2013

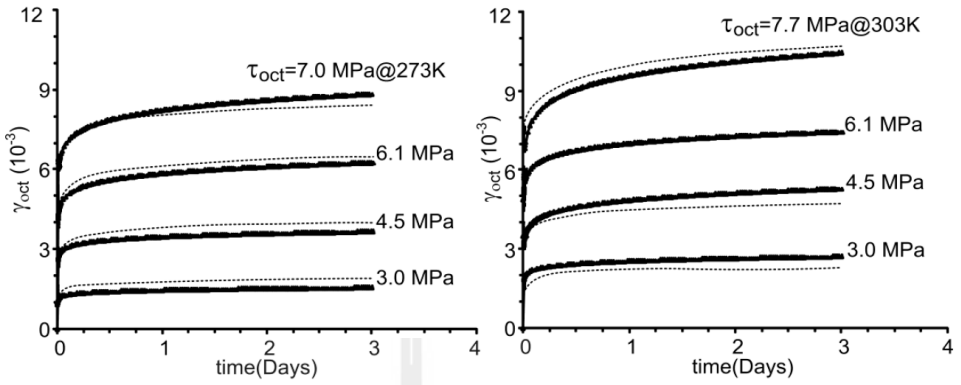

Figure 8. Octahedral shear strain-time curves for transient creep phase during the first 3 days.

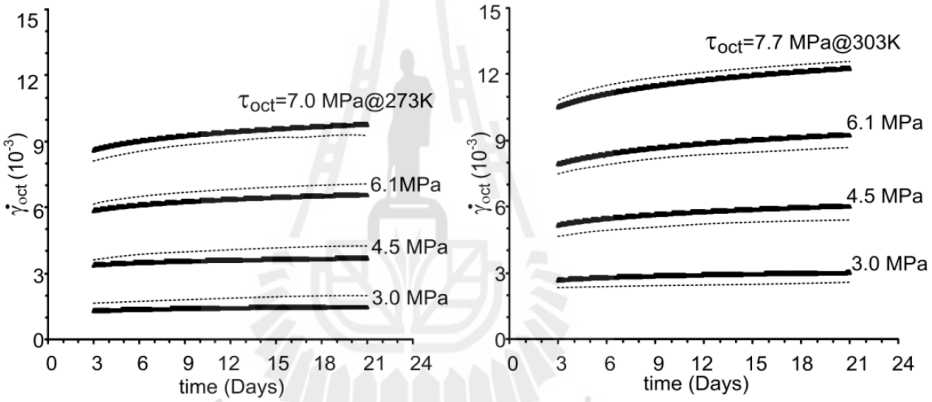

Figure 9. Octahedral shear strain-time curves for steady-state creep phase.

Table 1. Creep parameters.

Creep parameters	Transient creep phase	Steady-state creep phase
α, κ	1.238	1.890
β	1.581	1.620
γ	0.063	0.072
λ	347.267	493.468
A	-21.5×10^{-3}	-
B	16.200	-
R^2	0.967	0.964

where E is elastic modulus, ν is Poisson's ratio, σ_r is radial stress, σ_θ is tangential stress, σ^* is equivalent stress, S_r is deviatoric radial stresses, P_i, P_o are constant internal and external pressure, R is radial salt cavern, r is radial coordinate (R = r) (see Table 2).

Figure 10 shows the radial strains as function of time. The low temperature induces a lower strain and hence the total closure (radial strain) at the wall of storage cavern will also reduce.

Table 2. Salt properties used in the closure calculation.

Salt Properties		Sources
E	21.5 GPa	Phueakphum & Fuenkajorn (2010)
ν	0.4	Phueakphum & Fuenkajorn (2010)
P_i	3 MPa	assumed
P_o	20 MPa	assumed
R	25 m	assumed
r	25 m	assumed

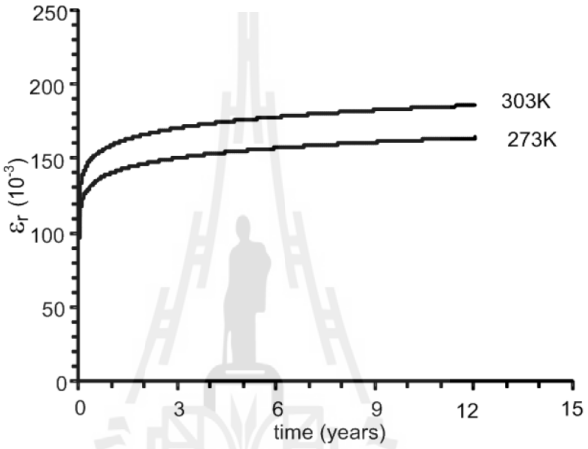

Figure 10. Radial strains (at the inner wall) as function of time, under temperatures of 273 K and 303 K.

5 DISCUSSIONS AND CONCLUSION

The test results indicate that the creep deformation increase with the temperatures. The test results show the transient creep phase of low temperature decreases with time and tend to be constant at steady-state creep phase. The exponential creep law agrees well with the test results in terms of the octahedral shear strains as a function of time. More testing is required to assess the effects of the low temperatures under a wider range of the applied octahedral shear stresses and confinements.

ACKNOWLEDGEMENT

This study is funded by Suranaree University of Technology and by the Higher Education Promotion and National Research University of Thailand. We would like to thank Pimai Salt Co. and Asean Potash Mining Public Co. who donate salt cores for testing.

REFERENCES

ASTM Standard D4543. 2008. Standard practice for preparing rock core specimens and determining dimensional and shape tolerances. *Annual Book of ASTM Standards,* Philadelphia, American Society for Testing and Materials. 1.

ASTM Standard D7070. 2008. Standard practice for creep of rock core under constant stress and temperature. *Annual Book of ASTM Standards*, West Conshohocken, PA.

Bachu, S. & Dusseault, M.B. 2005. Underground injection of carbon dioxide in salt beds. *Developments in Water Science*. 52: 637-648.

Bradley, R.A., Watts, E.C. & Williams, E.R. 1991. Limitting net greenhouse gas emission in the U.S. *Report to the US congress*. United States, 368 p.

Charpentier, J-P. 1984. Creep of rock salt elevated temperature. In *Proceeding of the second conference on the Mechanics Behavior of salt*. Clausthal, Germany. pp. 131-136.

Durham, W.B., Olgaard, D.L., Urai, J.L. & Schoenherr, J. 2008. Creep of rocksalt at low temperatures. In *the conference of 42nd U.S. Rock Mechanics Symposium (USRMS) June 29 - July 2, 2008*. San Francisco, CA. pp. 387-394.

Dusseault, M.B., Bachu, S. & Davidson, B.C. 2001. Carbon dioxide sequestration potential in salt solution caverns in Alterta. *Proceedings 2001 SMRI Fall Meeting*. Canada.

Obert, L. & Duvall, W. I. 1967. *Rock mechanics and the design of structures in rock*. Journal of the Franklin Institute. New York.

Phueakphum, D. & Fuenkajorn, K. 2010. Effects of cyclic loading on mechanical properties of Maha Sarakham salt. *Engineering Geology*. 112(1-4): 43-52.

Rutqvist, J. 2012. The geomechanics of co2 storage in deep sedimentary formations. *Geotech Geol Eng*. 30: 525-551.

Samsri, P., Sriapai, T., Walsri ,C. & Fuenkajorn, K. 2011. Polyaxial creep testing of rock salt. In *Proceedings of the Third Thailand Symposium on Rock Mechanics*. March 10-11, Springfield @ sea resort and spa, Cha-am, Suranaree University of Technology, pp. 125-132.

Senseny, P. E. 1983. *Review of constitutive laws used to describe the creep of salt*. Battelle Memorial Institute. Columbus.

Strumane, R. & Dekeyser, W. 1959. Low temperature creep of rock salt single crystals. *Acta Metallurgica*. 7(7): 520-521.

Tek, M.R. 1989. Underground storage of natural gas: theory and practice. *Applied Sciences*. Kluwer, Boston. 171: 458 p.

Warren, J. 1999. *Evaporites: Their Evolution and Economics*. Blackwell Science. Oxford.

BIOGRAPHY

Miss Tidarat Khathipphathee was born on January 19, 1989 in Chaiyaphum province, Thailand. She received her Bachelor's Degree in Engineering (Geotechnology) from Suranaree University of Technology in 2010. For her post-graduate, she continued to study with a Master's degree in the Geological Engineering Program, Institute of Engineering, Suranaree university of Technology. During graduation, 2010-2012, she was a part time worker in position of research assistant at the Geomechanics Research Unit, Institute of Engineering, Suranaree University of Technology.